ISMRM Tutorial, Montreal 2011
Computational Anatomy for Subcortical Population Brain Analysis at 1mm resolution

http://www.cis.jhu.edu/education/tutorials.php

Michael I Miller mim@cis.jhu.edu
The Johns Hopkins University

Outline

- Bijective correspondence: Populations studied via 1-1 mappings to atlas coordinates (LDDMM)
- Atlas's: Individual and Population
- Statistics: Gaussian Random Fields
- Representation in anatomical coordinates: PCA and surface harmonics
- P-values, clustering, LDA in diseased cohorts

• Ashburner & Friston (2011) Diffeomorphic registration using geodesic shooting and Gauss–Newton optimisation. Neuroimage 55:954-967
•Beg,Miller, Trouve, Younes, Computing Large Deformation Metric Mappings via Geodesic Flows of Diffeomorphisms,, Int. J. Comp. Vision, 2005.
•Christensen Miller Rabbitt, “Deformable Templates via Large Deformation Kinematics”, IEEE Transactions on Medical Imaging, 1997.
•Grenander, Miller, Computational Anatomy: An Emerging Discipline, Quarterly Applied Math. 1998.
•Khan, Wang, Beg (2008) FreeSurfer-initiated fully-automated subcortical brain sementation using Large Deformation Diffeomorphic Metric Mapping. Neuroimage 41: 735-746.
•Ma, Miller, Trouve, Younes, Template Estimation via EM Algorithm, Neuroimage, 2008.
• Miller, Trouve, Younes, On the Metrics and Euler Lagrange Equations of Computational Anatomy, Annual Review of Biomedical Engineering, 2002
•Miller, Trouve, Younes , Geodesic Shooting for Computational Anatomy, J. Math. Imag. And Vision, 2006.
•Oishi, Faria, van Zijl, Mori, MRI Atlas of Human White Matter, 2010 Academic Press

•Qiu, Miller "Multi-Structure Network Shape Analysis via Normal Momentum Maps", NeuroImage, 2008.
•Qui , Crocetti, Adler, Mahone, Denckla , Miller, Mostofsky (2009) Basal Ganglia Volume and Shape in Children With Attention Deficit Hyperactivity Disorder. Am. J. Psychiatry. 166: 74-82.
•Qiu, Brown, Fischl, Ma, Miller: Atlas Generation for Subcortical and Ventricular Structures With Its Applications in Shape Analysis. IEEE Trans. on Image Processing 19(6): 1539-1547 (2010)
•Qiu, Adler, Crocetti, Miller, Mostofsky, Basal Ganglia Skills Predict Social Communication and Motor Dysfunction in Boys with Spectrum Function Disorder. J. Am. Acad. Child Adolescent Psychiatry 2010 June 49(6):539-551
•Smith, Wang, Cronenwett, Mamah, Barch, Csernansky (2011) Thalamic morphology in schizophrenia and schizoaffective disorder. J. Psychiatric Research, 45: 378-385
•Thompson & Apostolova (2007) Computational anatomic methods as applied to aging and dementia. Brit. J. Radiology 80: S78-S91
•Vaillant, Miller, Trouve, Younes, Neuroimage 2005
• Vercauteren, Pennec, Perchant & Ayache (2009) Diffeomorphic demons: efficient non-parametric image registration. Neuroimage 45: S61-S72
•Wang, Lee, Bailey, Hartlein, Gado, Miller & Black (2007). Validity of large-deformation high dimensional brain mapping of the basal ganglia in adults with Tourette syndrome. Psychiatry Research: Neuroimaging. 154: 181-190.

Computational Functional Anatomy
is the study of structure and function response variables in populations.

Populations are studied via statistics in the template coordinate systems.

Bijective correspondences are used to carry information from one coordinate system to another - we call these bijections diffeomorphisms.

Populations often involve many modalities: B0, FA, T1, T2, Segmentations,…

Bijective correspondence via diffeomorphic mapping

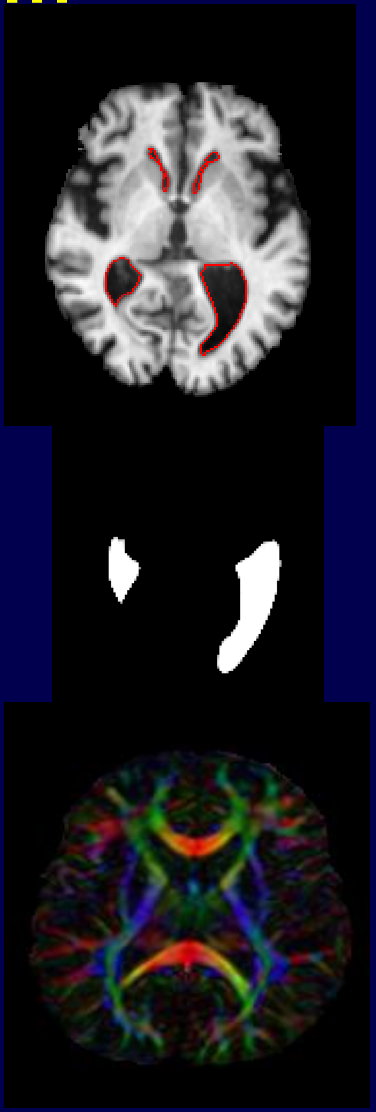

Atlas: Electronic form of anatomical knowledge

Patient data

Bijective mapping goes forwards and backwards.

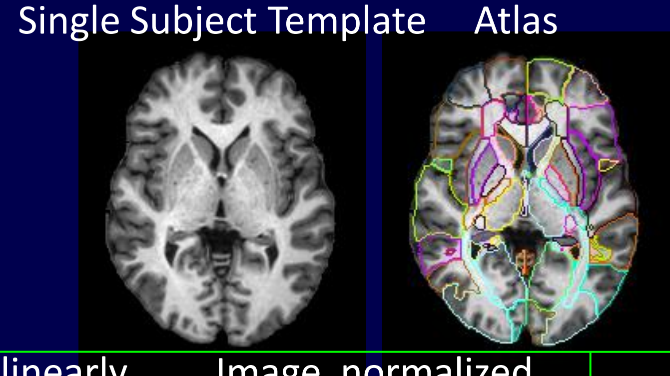

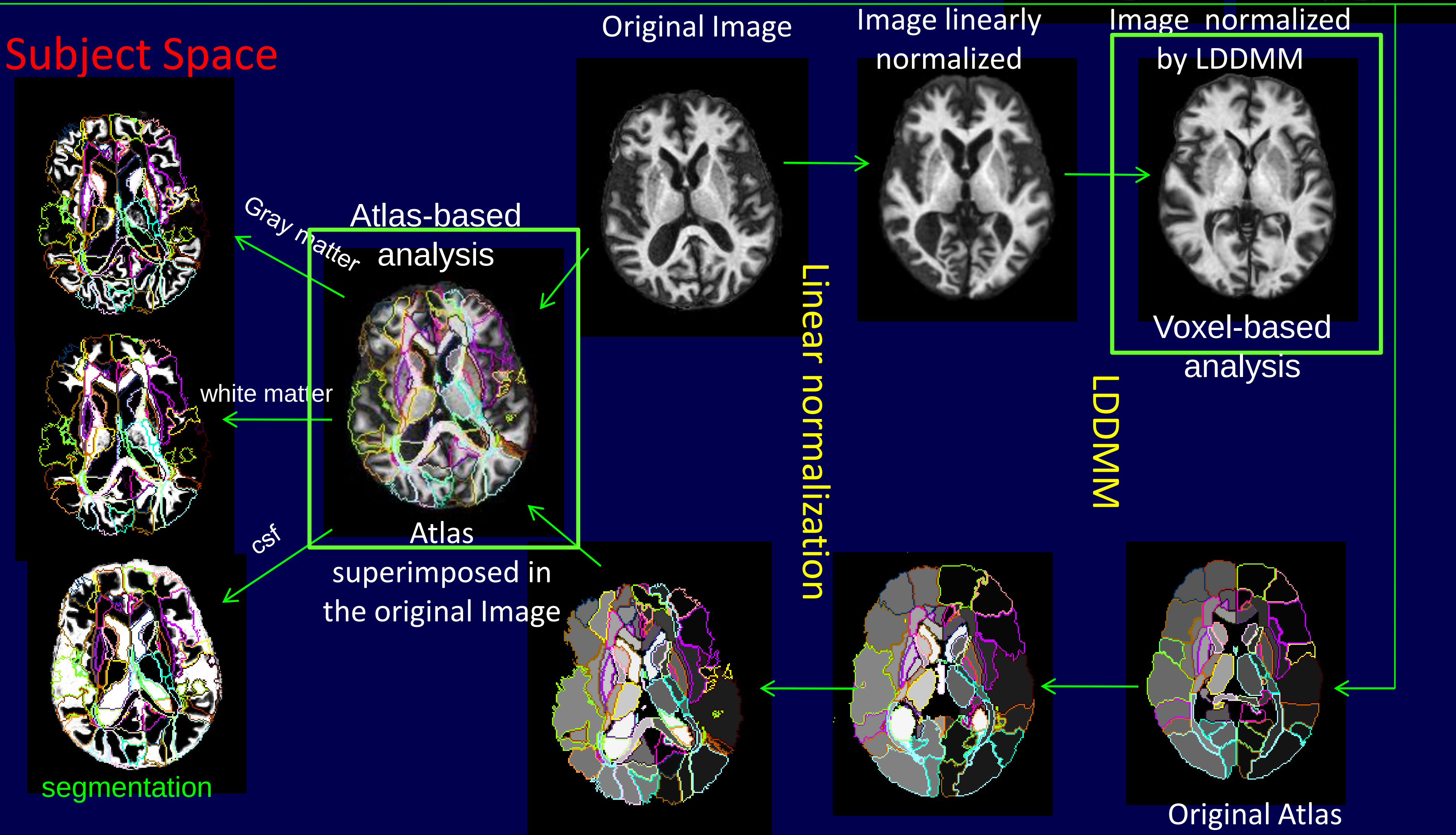

The current state of the art structural validity for subcortical structures in 1mm scale MRI.

Kappa ~0.8 Overlap of Subcortical Structures Blue=LDDMM

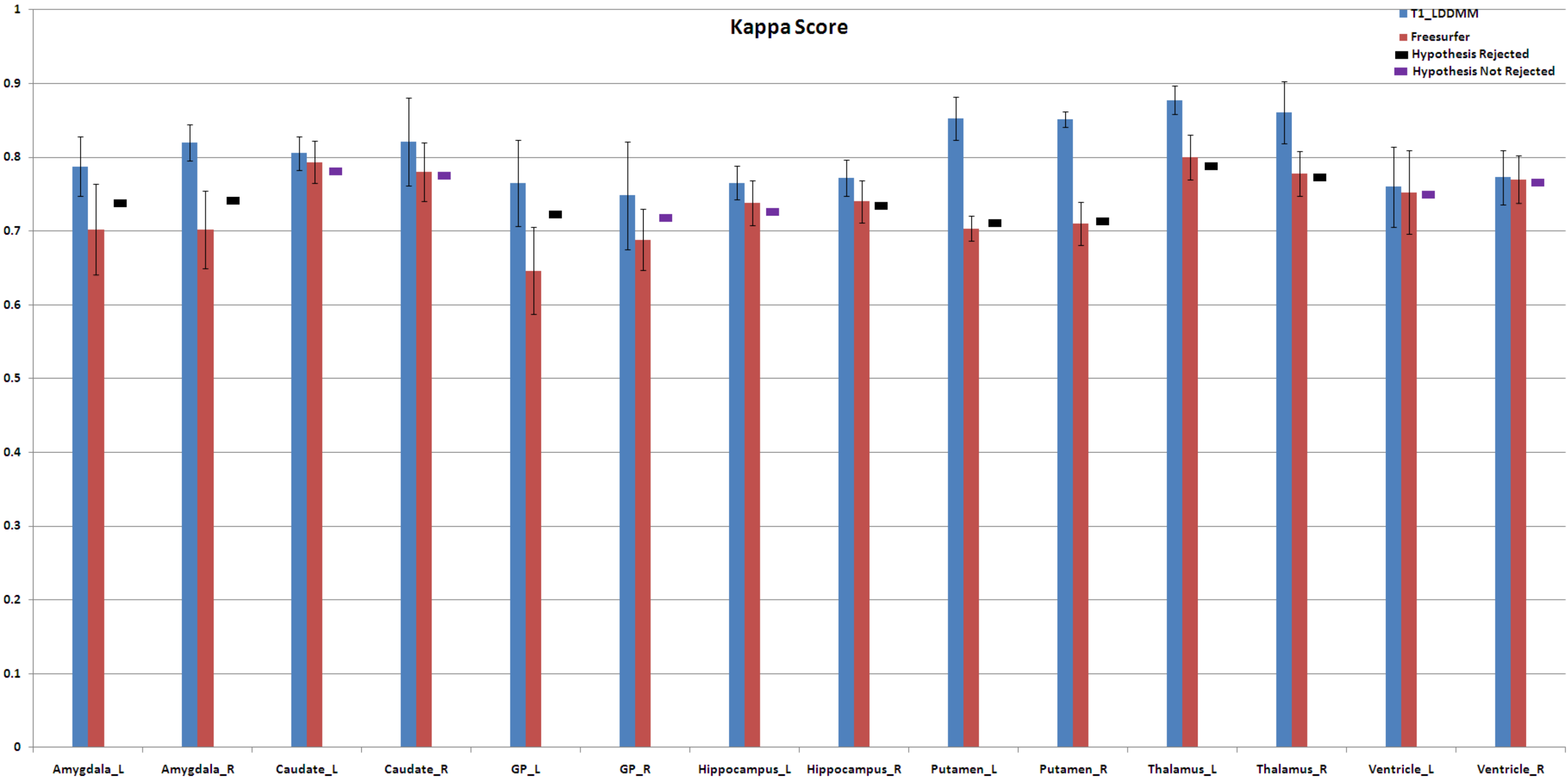

Volume Bias ~10%
Blue=LDDMM

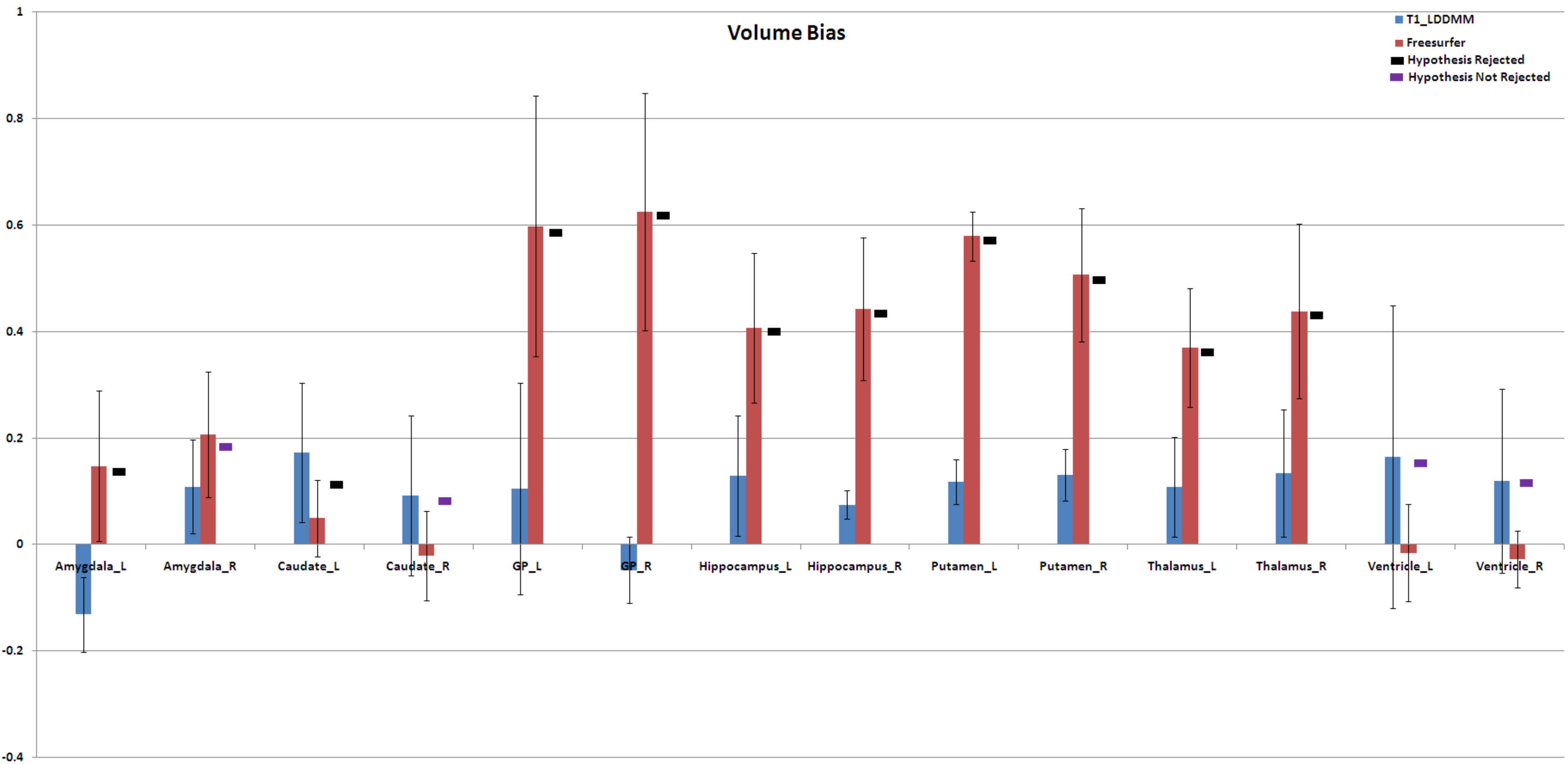

Populations are studied via templates with statistics encoded in template coordinates.

Templates encode populations via bijections.

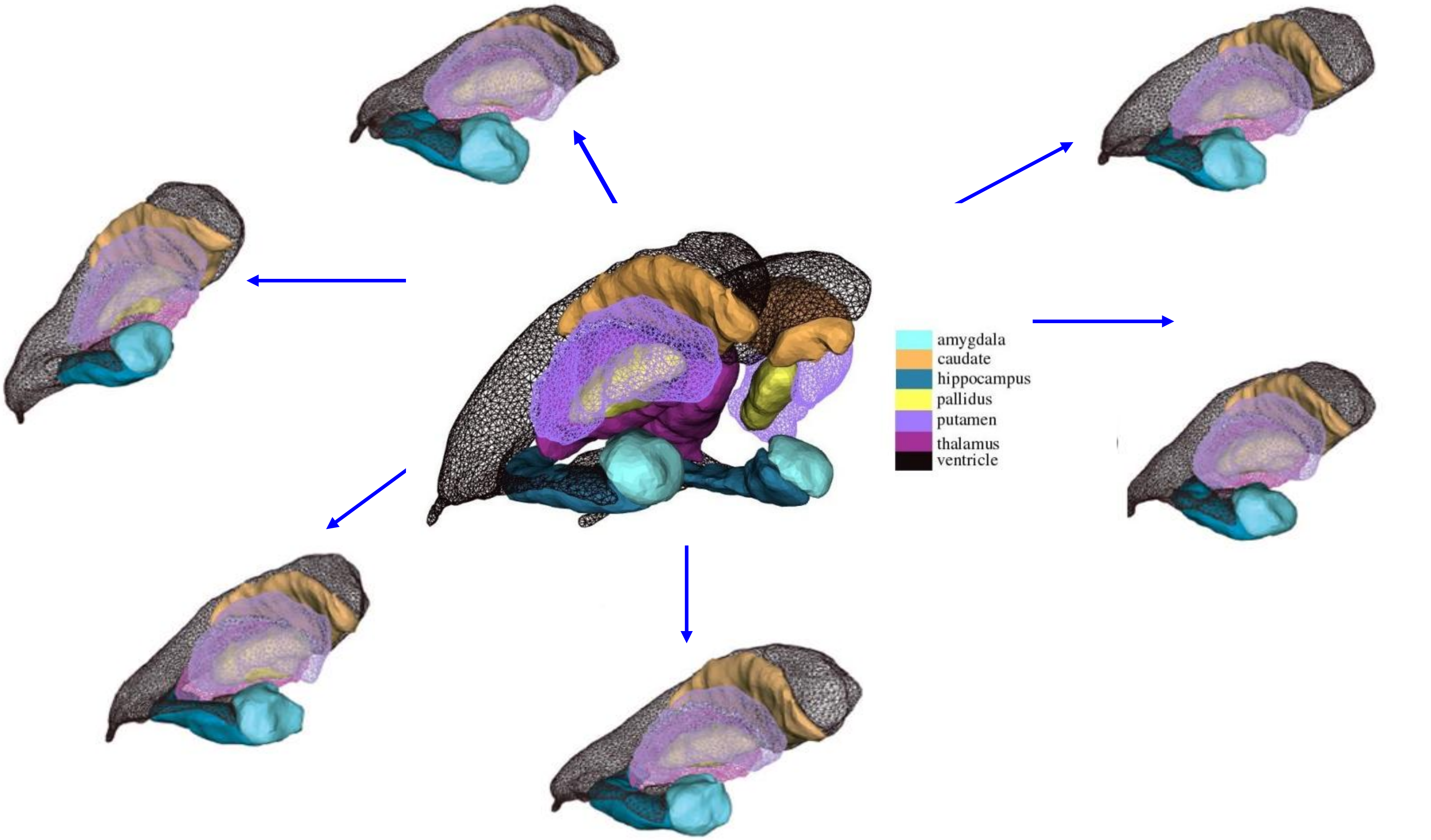

Bijective correspondences are generated via large deformation metric mapping (LDDMM) which are flows of the Euler-Lagrange equations.

-bijection is generalization of translations, rotations, scales to infinite dimensions

Bijections are computed via Euler-Lagrange flow equations.

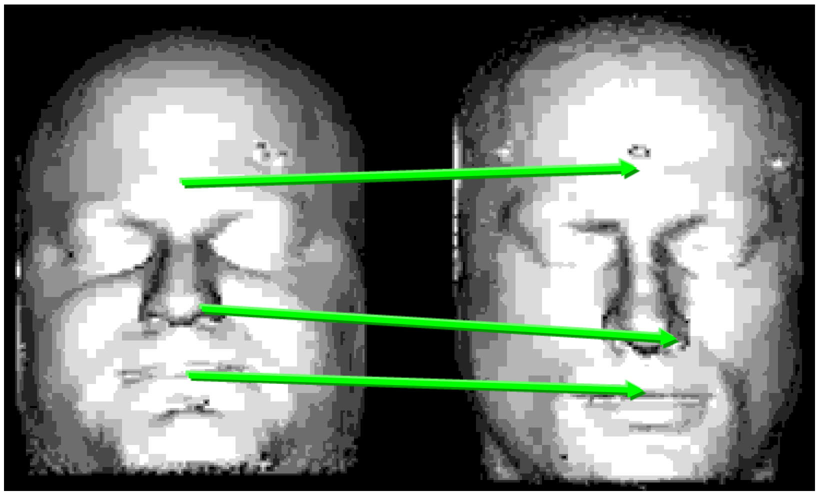

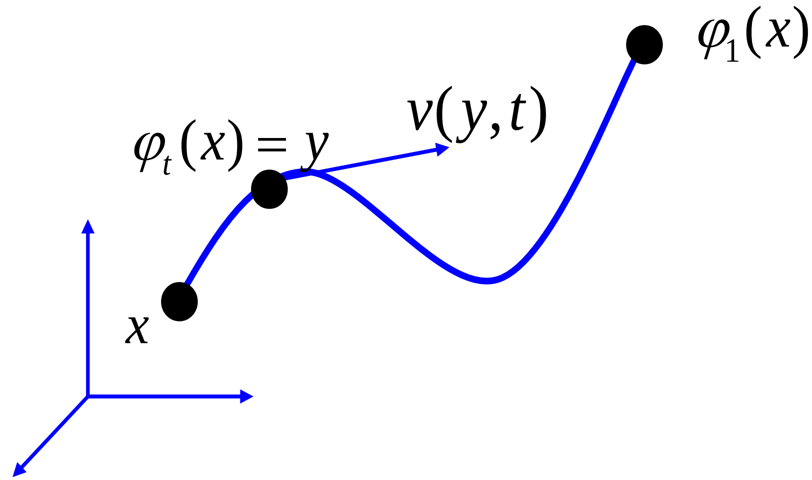

Lagrangian $$\dot{\varphi}_t(x) = v_t(\varphi_t(x)), \varphi_0 = id$$

Eulerian $$\dot{\varphi}_t^{-1}(x) = -D\varphi_t^{-1}(x) v_t(x), \varphi_0^{-1} = id$$

D=Jacobian matrix $\left(\frac{\delta v_i}{\delta x_j}\right)$

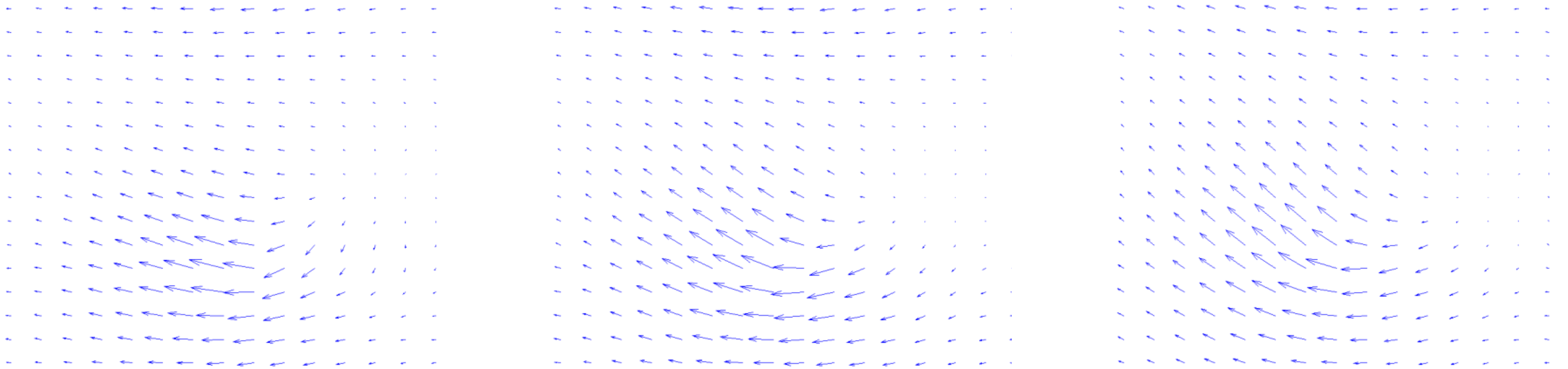

0 6 12

$$\dot{\varphi}_t(x) = v_t(\varphi_t(x))$$

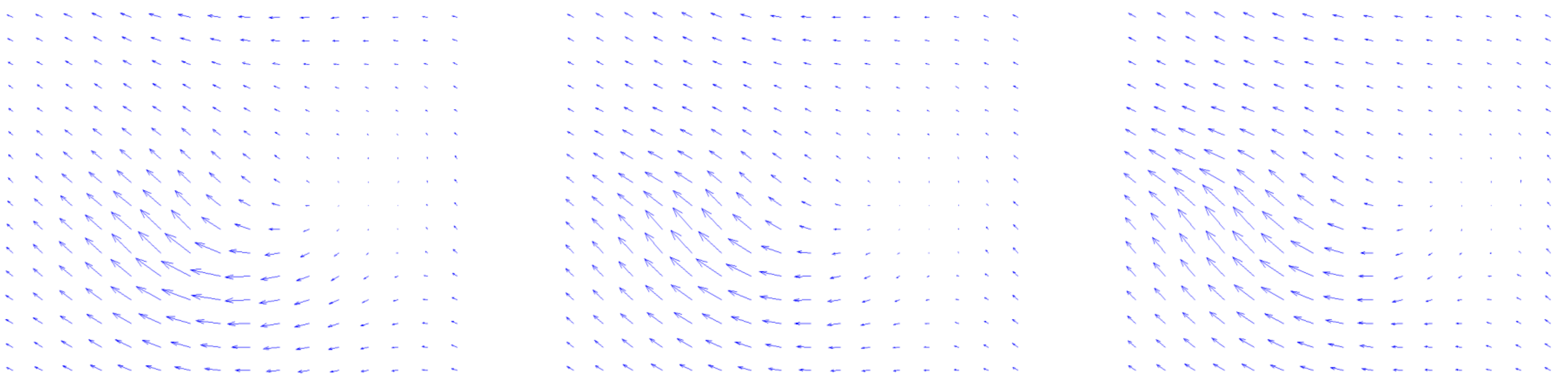

18 24 29

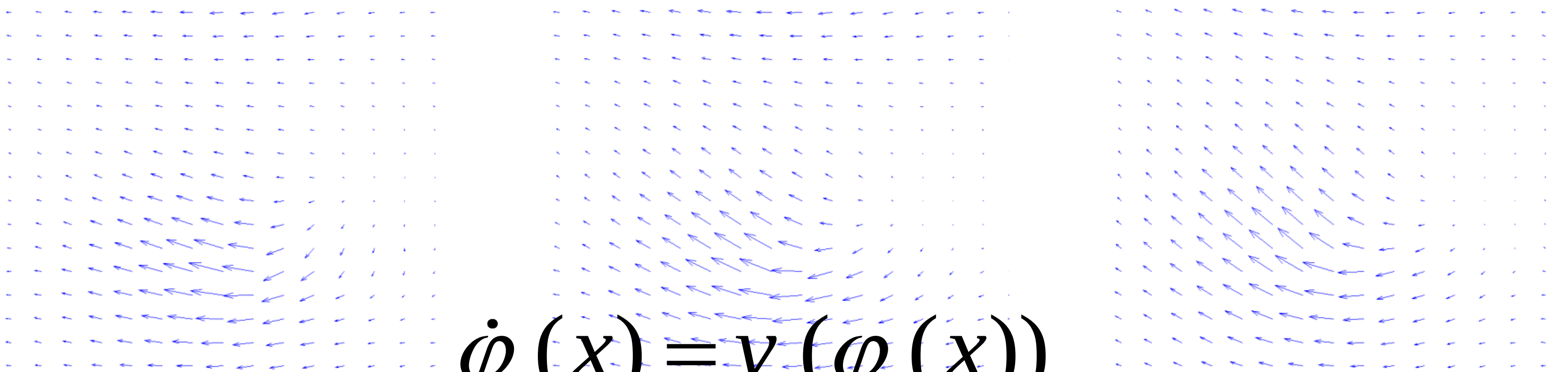

$$\dot{\varphi}_t(x) = v_t(\varphi_t(x))$$

$$I \circ \phi_t^{-1}$$

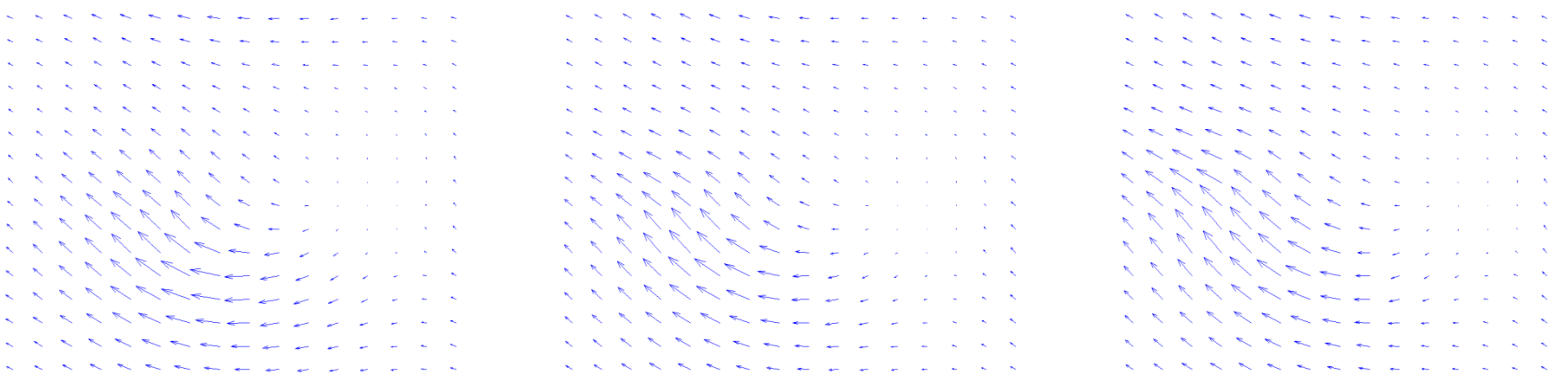

The Euler-Lagrange equations are used to constrain the generation of bijections because they support large – high dimensional - deformations which carry structures consistently:

- subvolumes to connected subvolumes
- surfaces to surfaces
- sulcal curves to sulcal curves

Bijective Euler-Lagrange Flows (Diffeomorphisms)

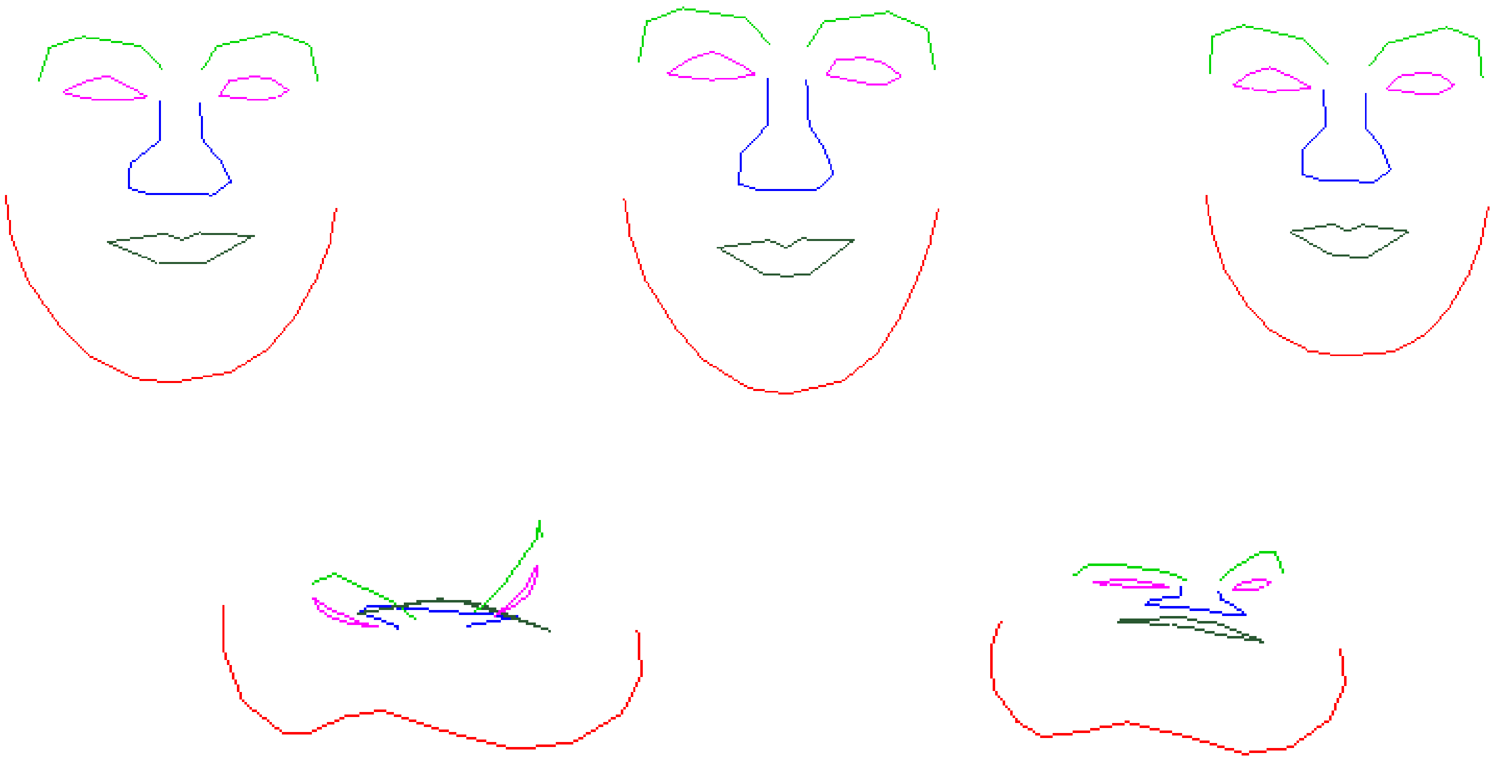

No Euler equation flow Euler equation flow

Simple example of large deformations in human anatomy

Closed lateral ventricles

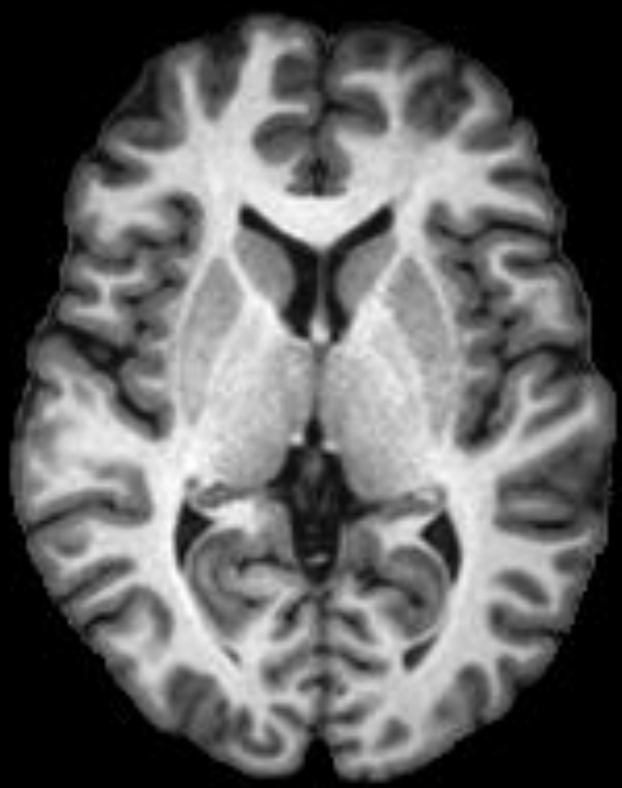

Expanded lateral ventricles

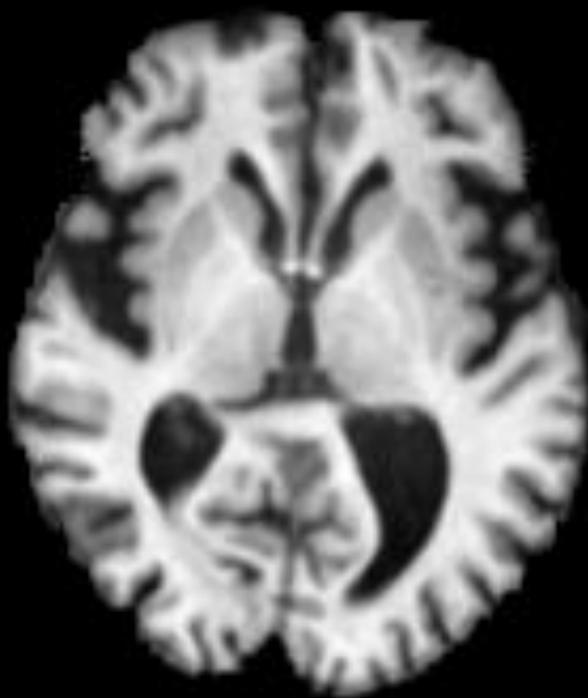

Bijective Mapping Available via MRIStudio
www.mristudio.org

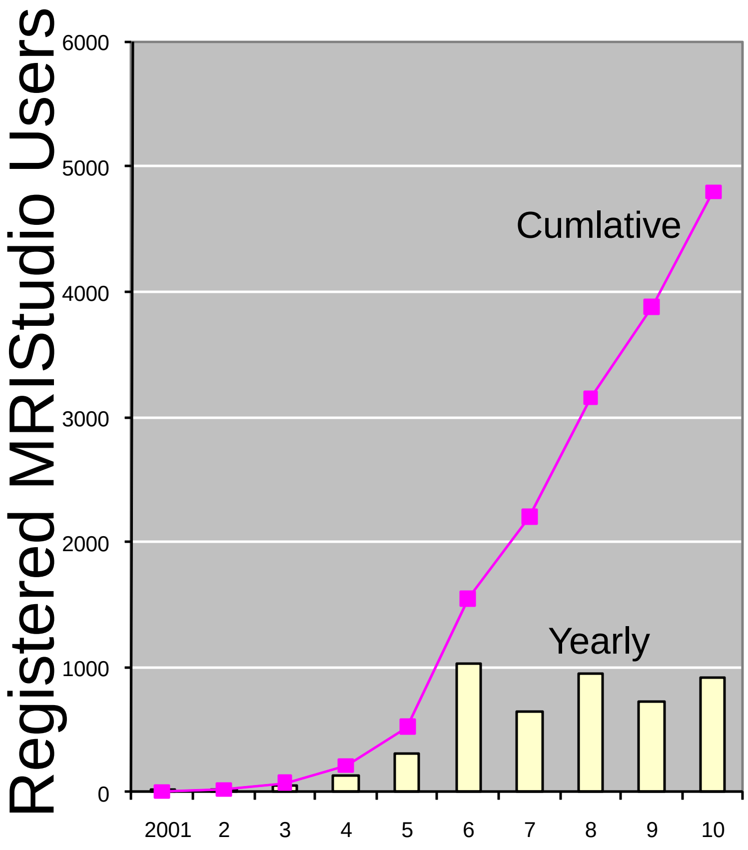

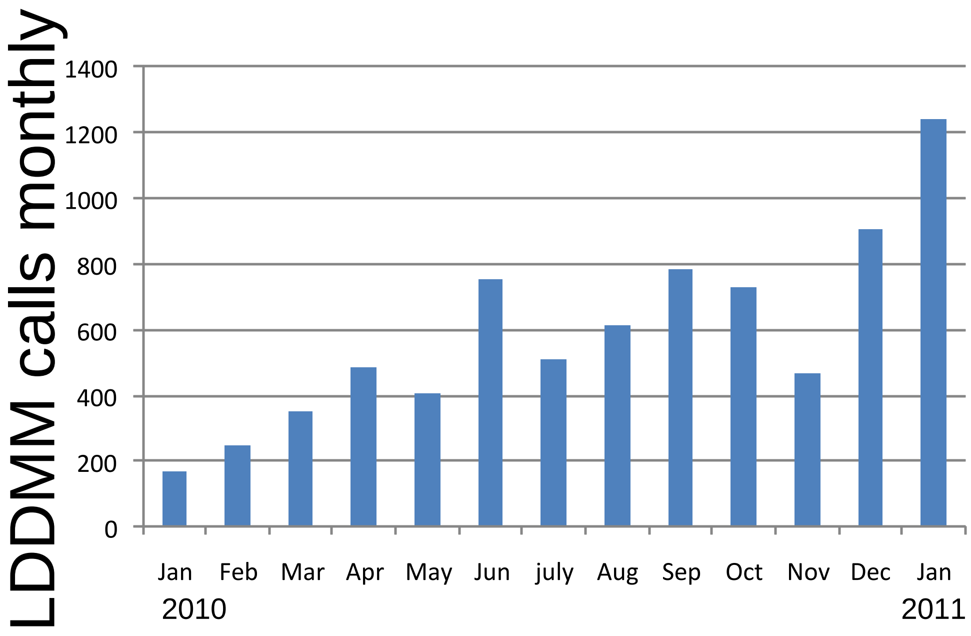

Individual Templates
and
Population Templates

JHU-MNI Atlas
www.mristudio.org

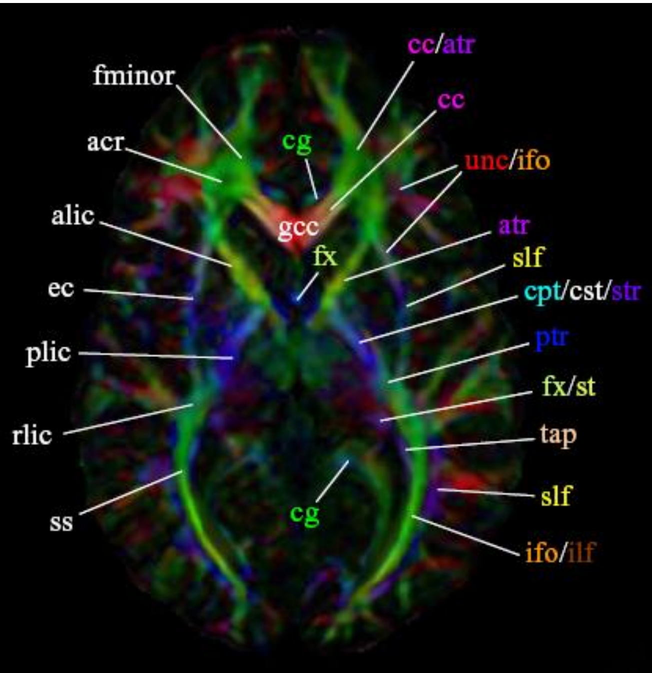

- Full segmentation (200 structures)
- Stereotaxic (MNI and Talairach)
- Gray / white matter assignment
- Modern Brodmann's map
- Population-averaged tract coordinates

LDDMM

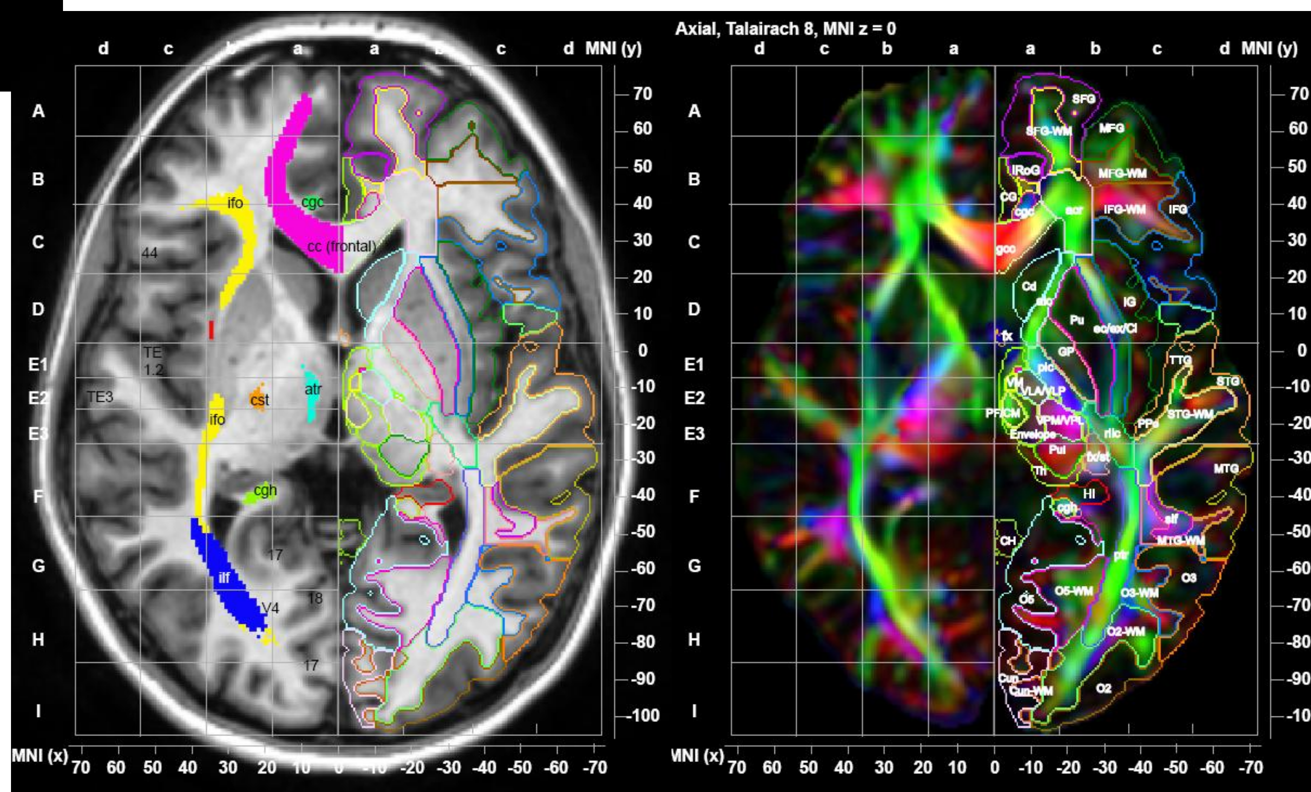

Building Population Atlases

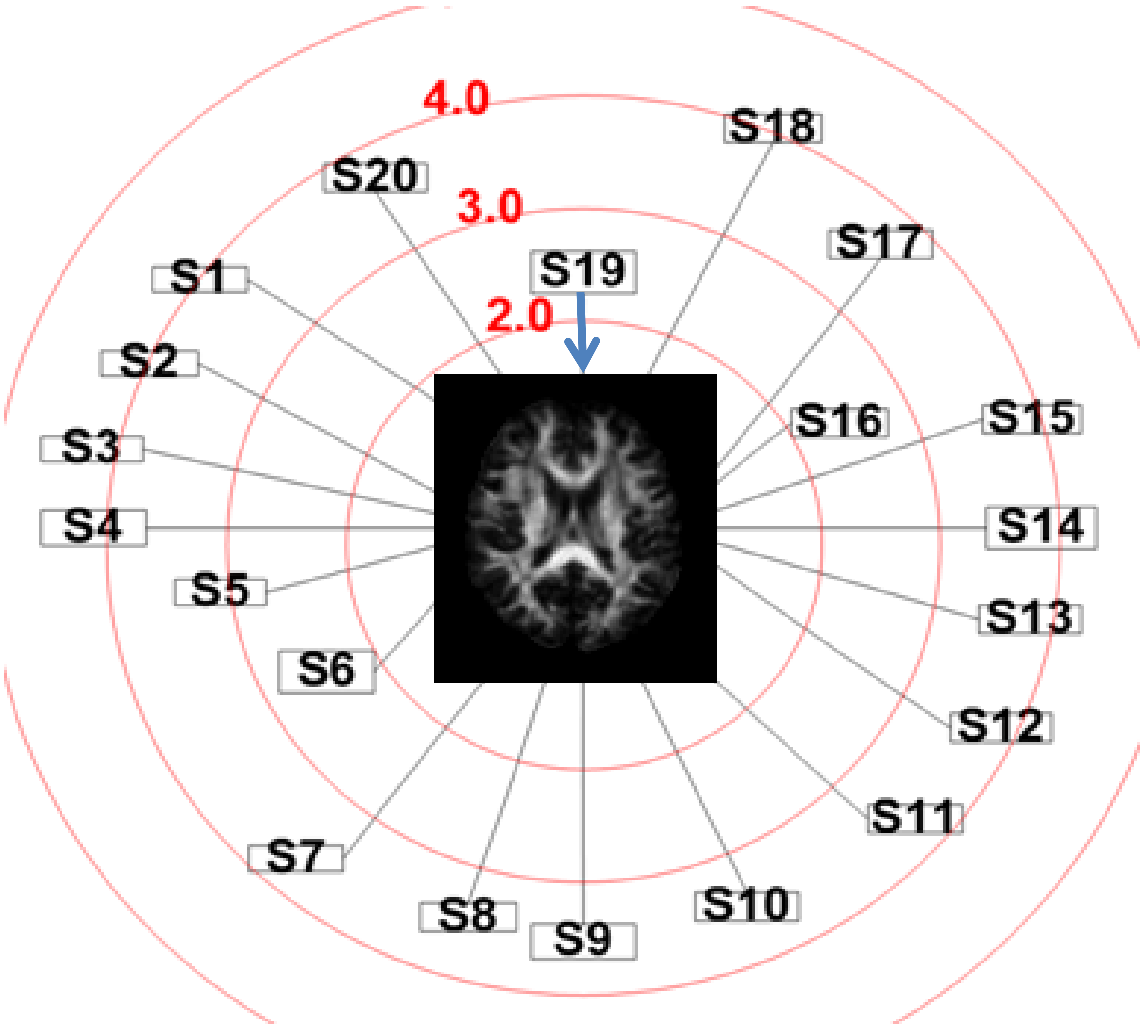

Population Atlas

Population based template generation via EM Algorithm

The template to be estimated is an unknown deformation of an anatomy in the "center" of a collection of human anatomies - indistinguishable from other anatomical configurations - not an arithmetic average.

The complete data are the deformations generating the (unknown) template mapping to the population data.

- E-step: generates the conditional mean deformations given the previous iterate **template-old** and the observed MRI imagery.

- M-step: generates **template-new** maximizing the complete-data posterior distribution with respect to the unknown deformation of **template-old**.

EM Algorithm- Iteration 1

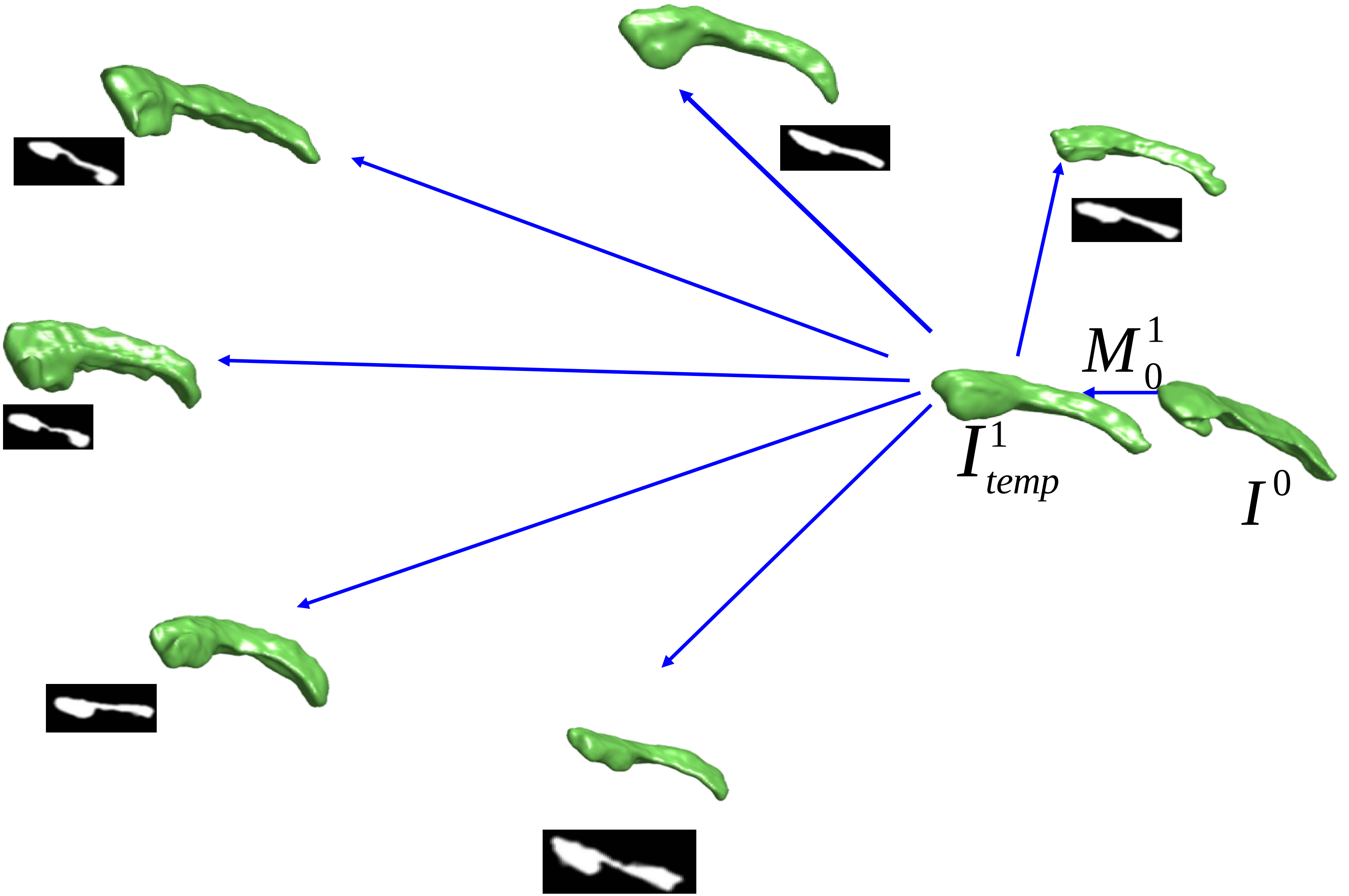

EM Algorithm: Iteration n

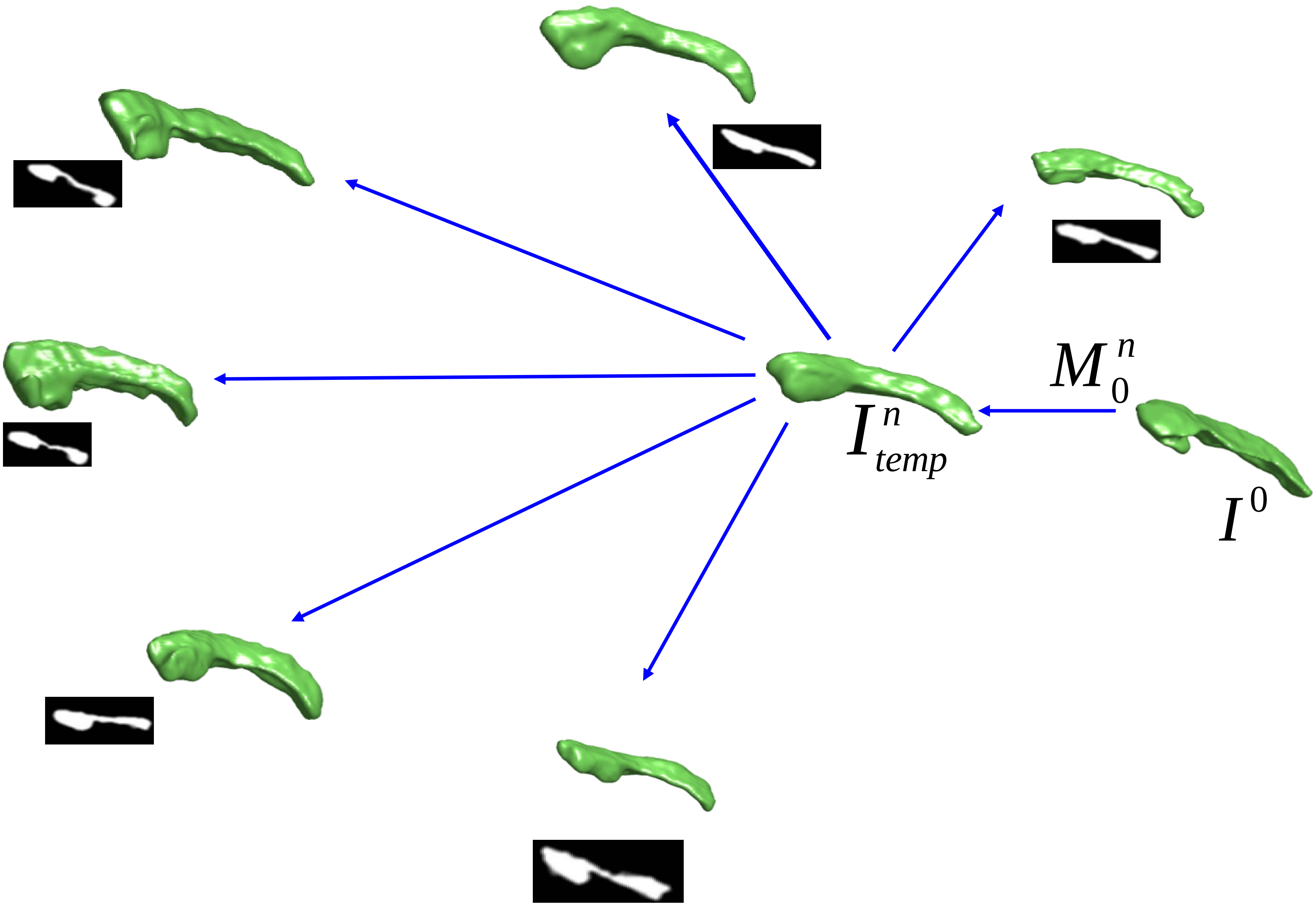

EM Algorithm: Convergence

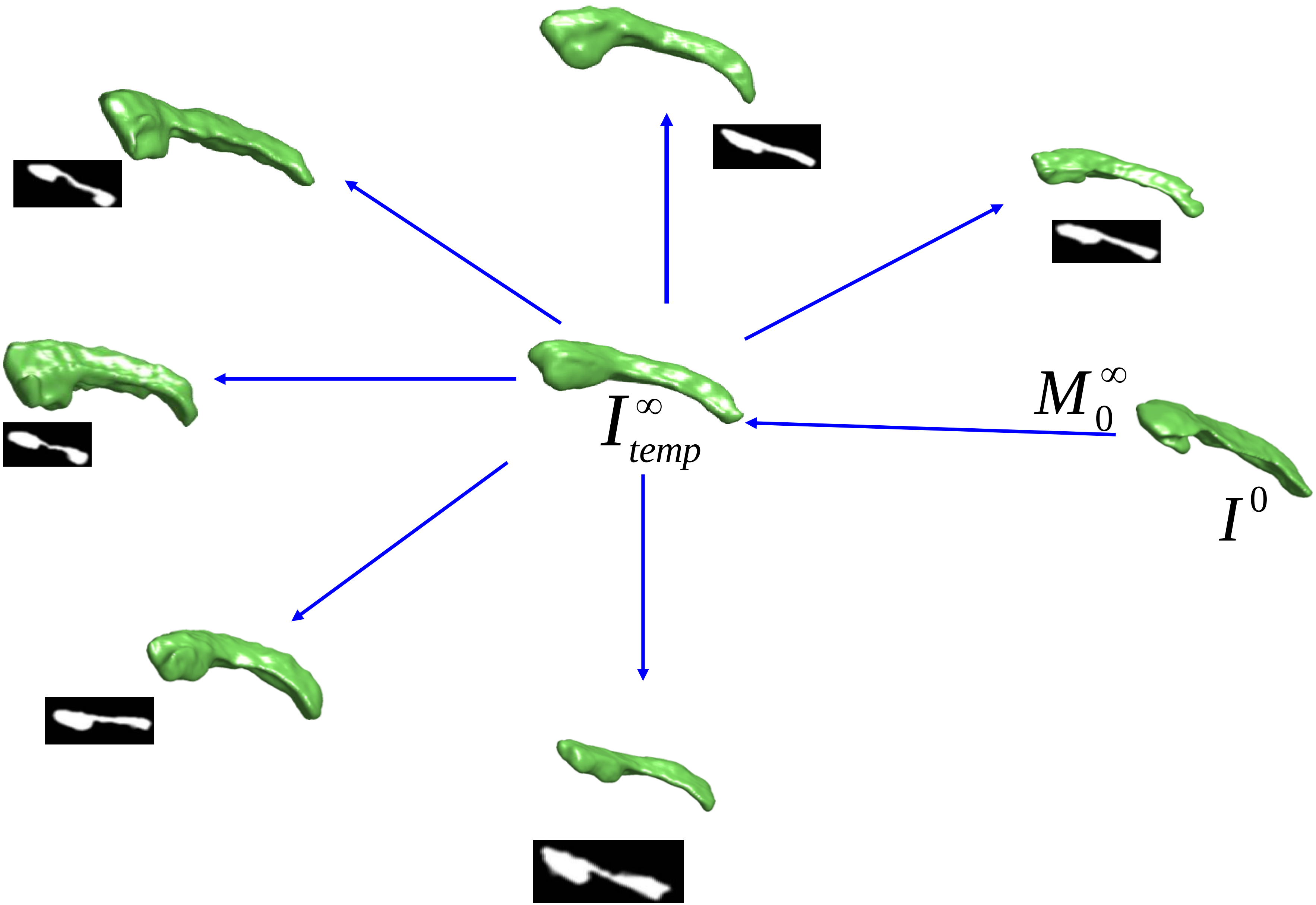

LDDMM Subcortical Atlas: An Example

https://caportal.cis.jhu.edu/pipelines/atlases/human

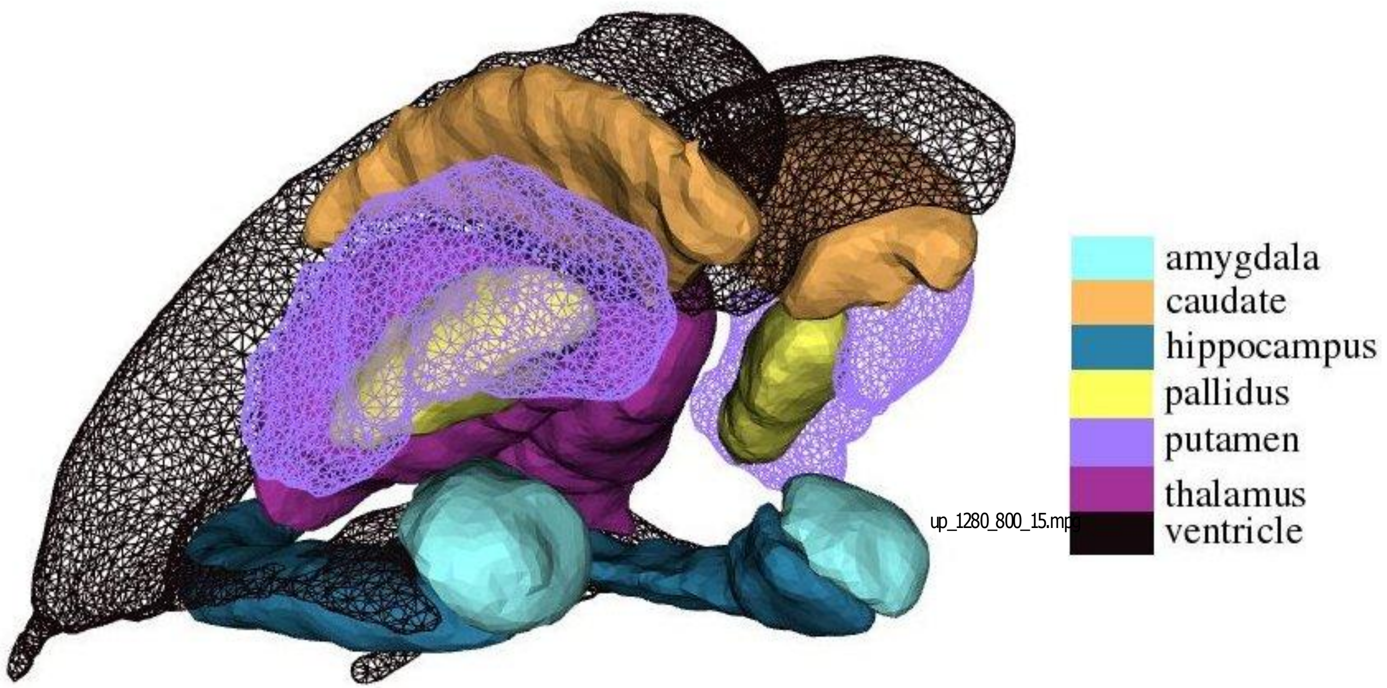

The atlas was built based on the manually labeled image volumes of 41 subjects using large deformation diffeomorphic metric template mapping algorithm. The population includes 10 young adults, 10 middle age adults, 10 healthy elders, and 11 Alzheimer's pateients.

Statistics for Populations

Statistics

Statistics are computed using Gaussian random fields on the response variables and complete orthonormal bases indexed over the anatomical coordinates.

Statistics are studied as pairs (F,M) of function F on manifolds M:

$$\left(\underset{\substack{Element\\ Hilbert\\ Space H(M)\\ with CON}}{F}, \underset{\substack{Anatomical\\ Manifold}}{M} \right)$$

Hilbert Space
H(M)
with a CON base.

- Statistics performed in the coordinates of M

- Statistics via GRF models in H(M)

$$F = \sum_k \underset{\substack{\text{structure-function}\\ \text{response-variables}}}{F_k} \underset{\substack{\text{Laplace-Beltrami or}\\ \text{PCA CON Basis}}}{\phi_k}$$

Statistics are obtained via template injection onto the targets. The bijection encodes in template coordinates the target shapes.

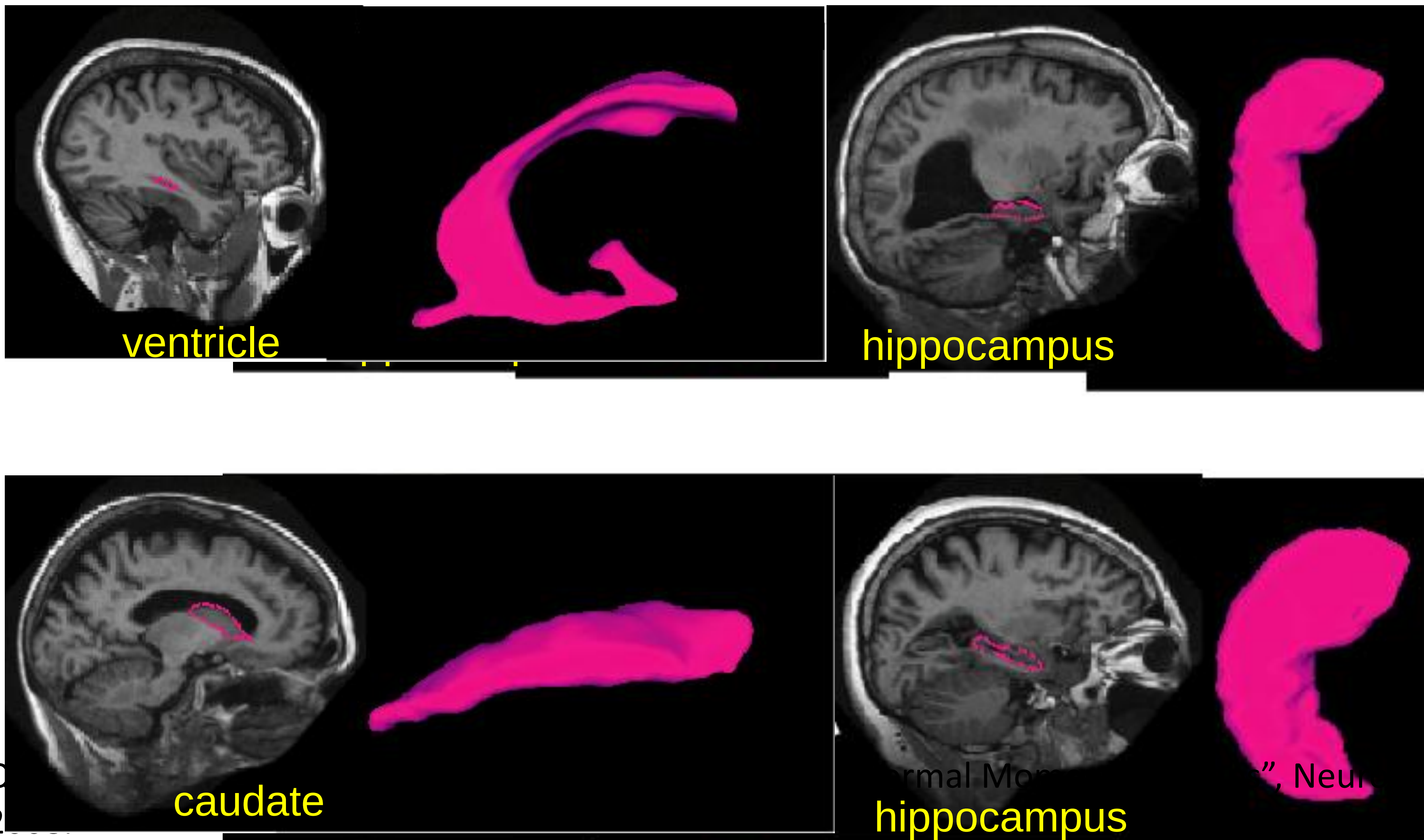

PREDICT STUDY: template structures carry a set of response variables and surface expansion functions.

$$F = \sum_k F_k \phi_k$$

response-variables

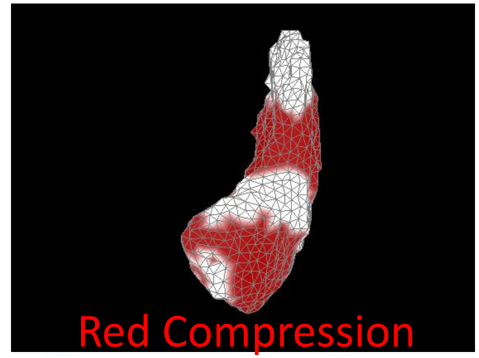

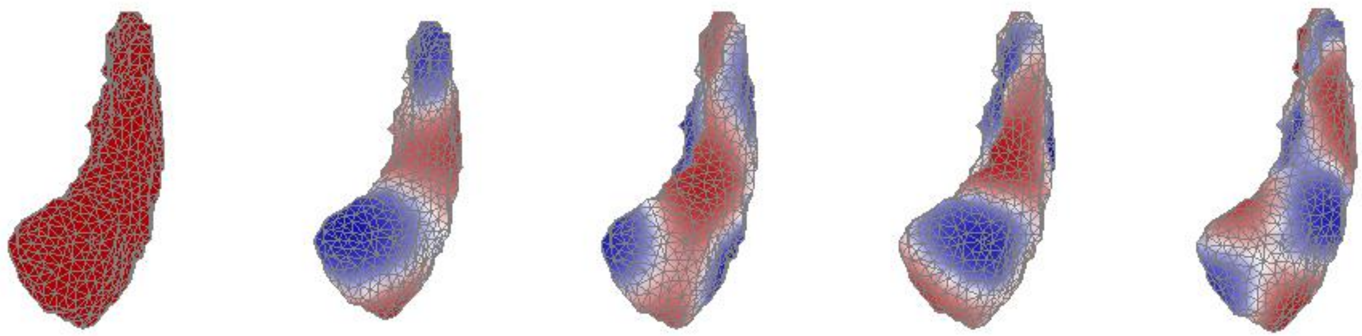

Five expansion functions on the template.

A response variable Fk can be generated by taking the Jacobian determinant of the template bijection onto the target and projecting onto the basis.

The Atlas to Target Statistical Pipeline

MRI Target

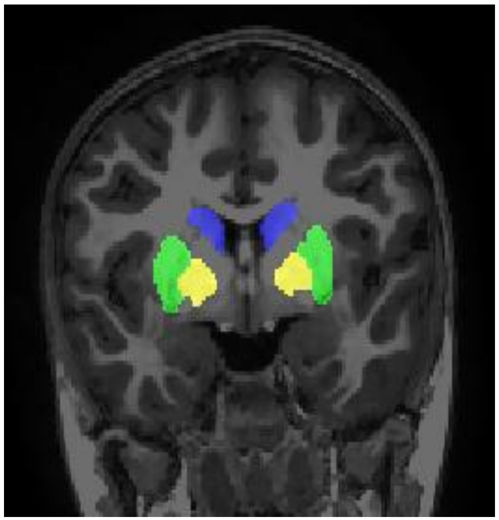

Template

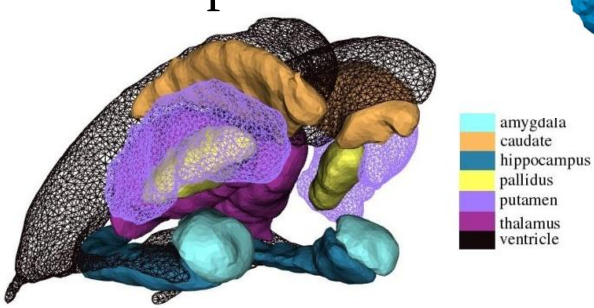

Putamen Template Injected into Targets

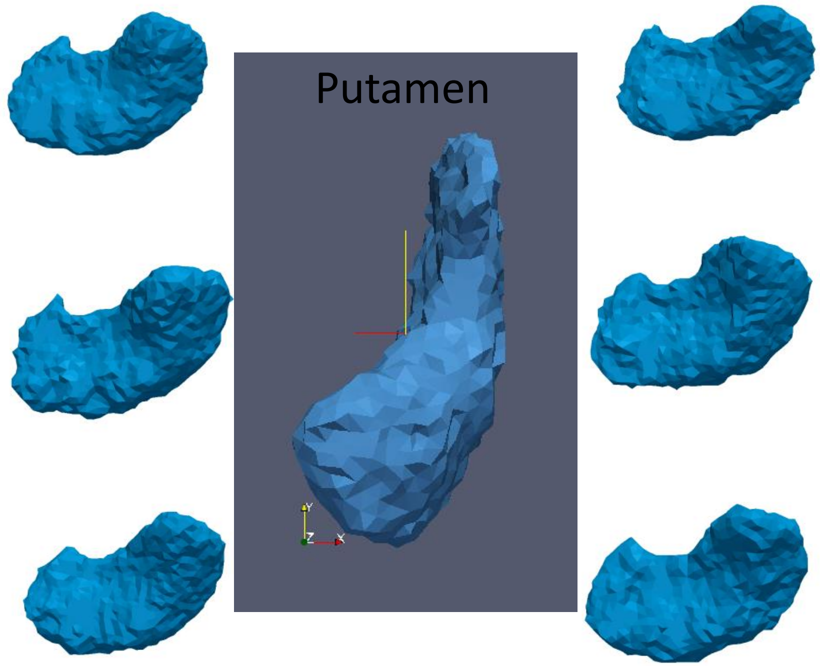

Shape Encoded on Template Surface Structures via Random Field Models

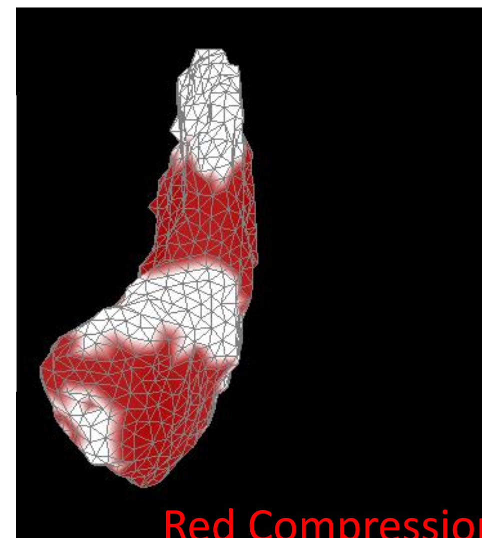

$$F = \sum_k F_k \phi_k$$

F_k: structure-function response-variables

ϕ_k: Laplace-Beltrami or PCA Basis

The Atlas to Target Statistical Pipeline

MRI Target

Template

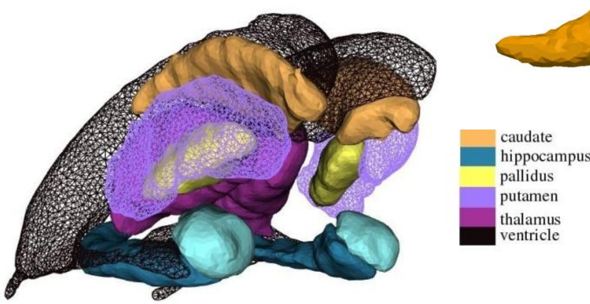

Caudate Template Injected into Targets

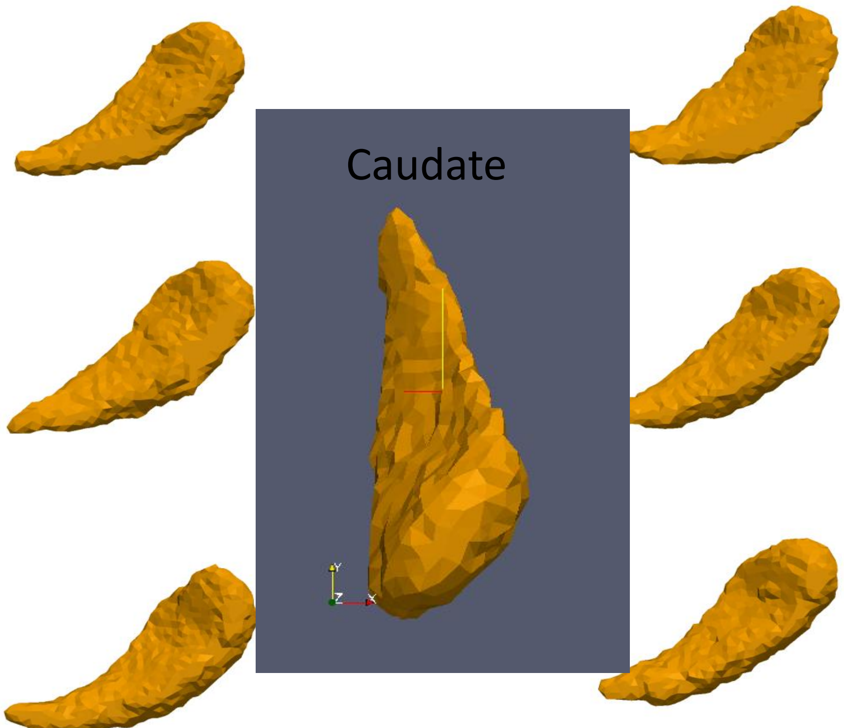

Shape Encoded on Template Surface Structures via Random Field Models

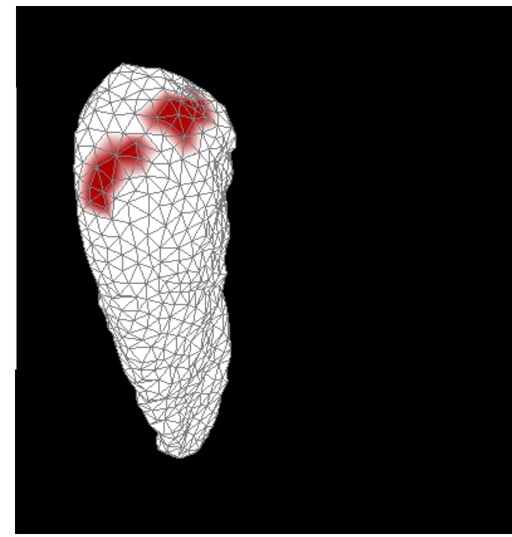

$$F = \sum_k F_k \phi_k$$

F_k: structure-function response-variables

ϕ_k: Laplace-Beltrami or PCA Basis

The PREDICT Study: An Example of Subcortical Shape Analysis

Human striatal studies of HD patients

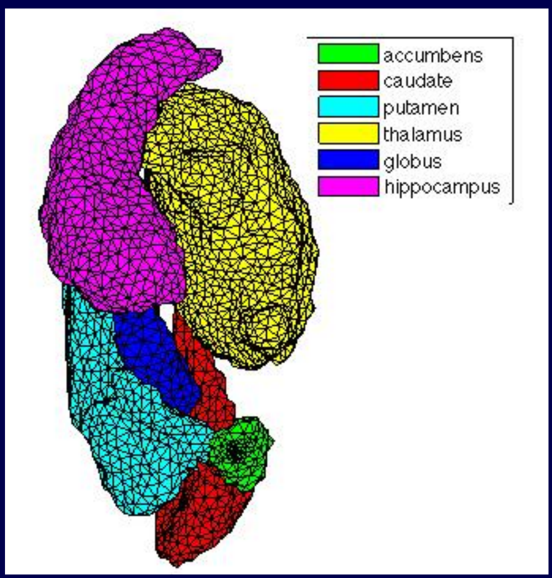

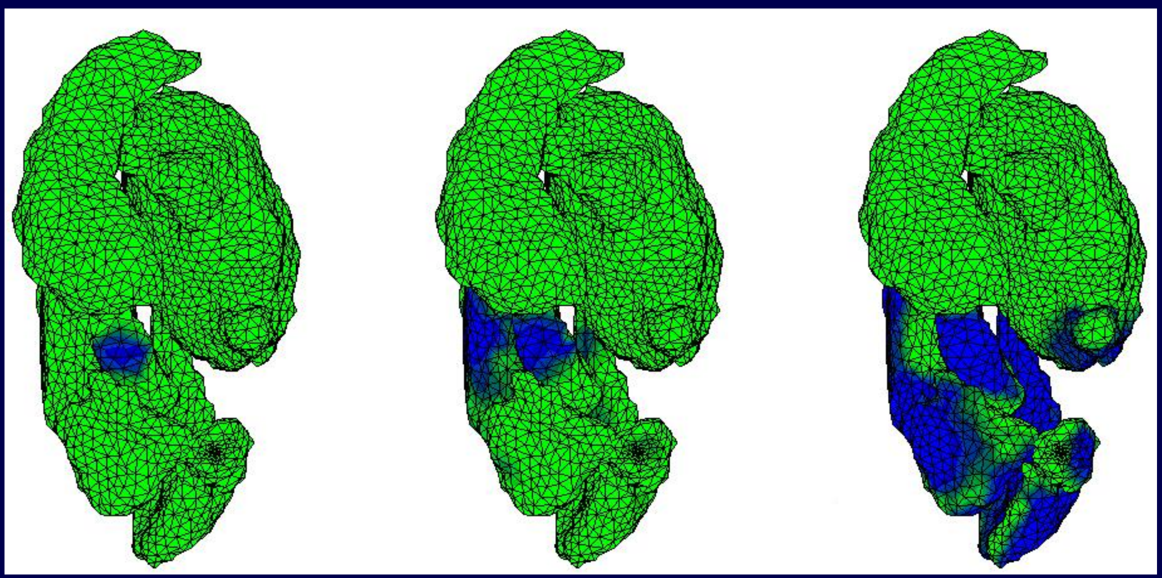

Far from onset

Close to onset

Early affected

Younes, Paulsen, Ross, et. All.,Heterogeneous atrophy of subcortical structures in prodromal HD as revealed by statistical shape analysis, submitted.

Curved Coordinate System Representations via an Orthonormal Basis

PCA and Surface Harmonics

$$F = \sum_k F_k \phi_k$$

structure-function response-variables (F_k)

Laplace-Beltrami or PCA Basis (ϕ_k)

PCA, one orthonormal base in Anatomical Coordinates

Principle Components are an orthonormal basis which can be used, requiring training data.

$$F = \sum_k F_k \phi_k$$

response-variables   PCA Basis

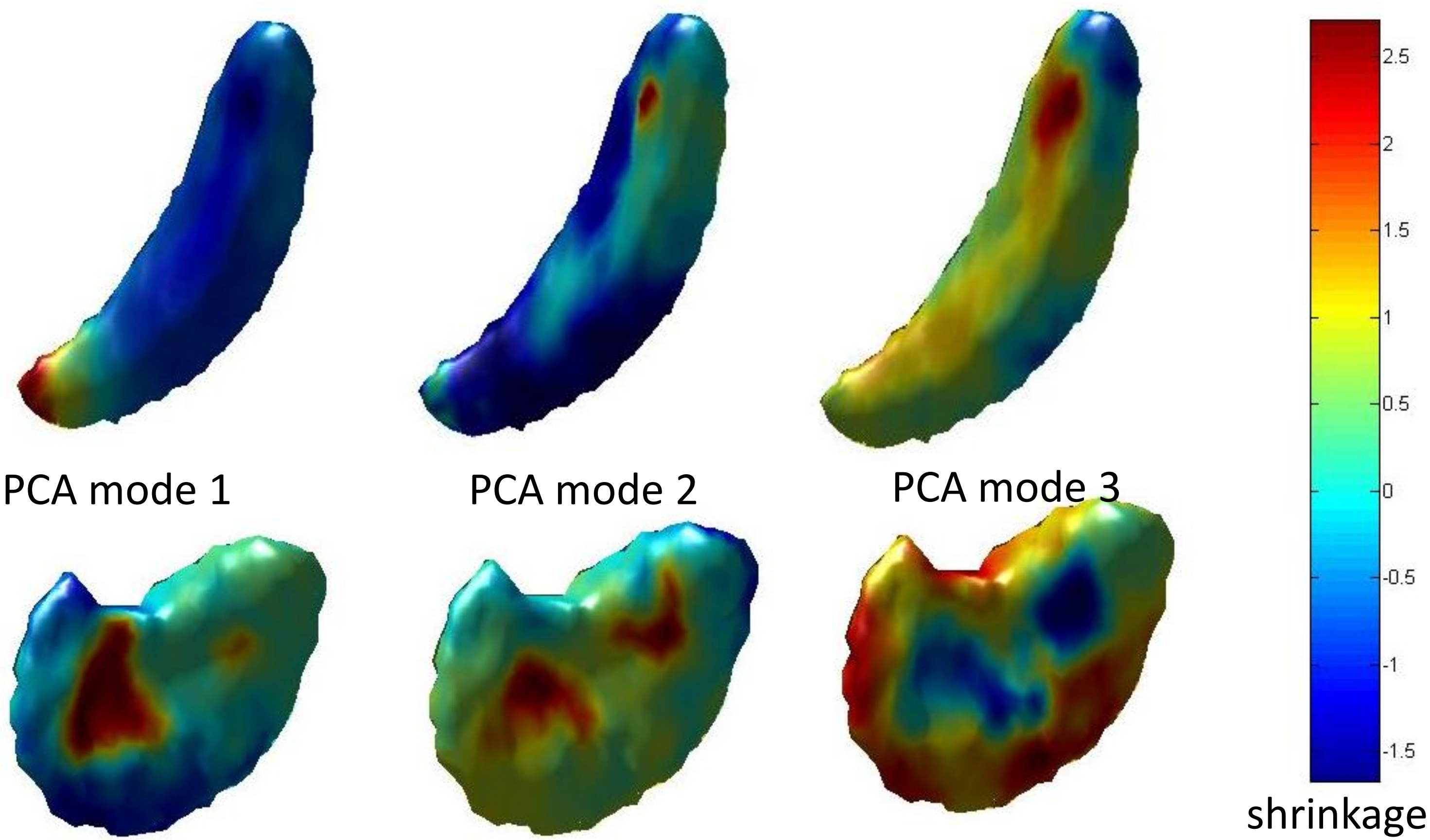

Laplace-Beltrami, another orthonormal base in anatomical coordinates not requiring training data (generalization of the Fourier basis)

Complete orthonormal bases via harmonics of the Laplacian operator; like the Fourier basis no training data required.

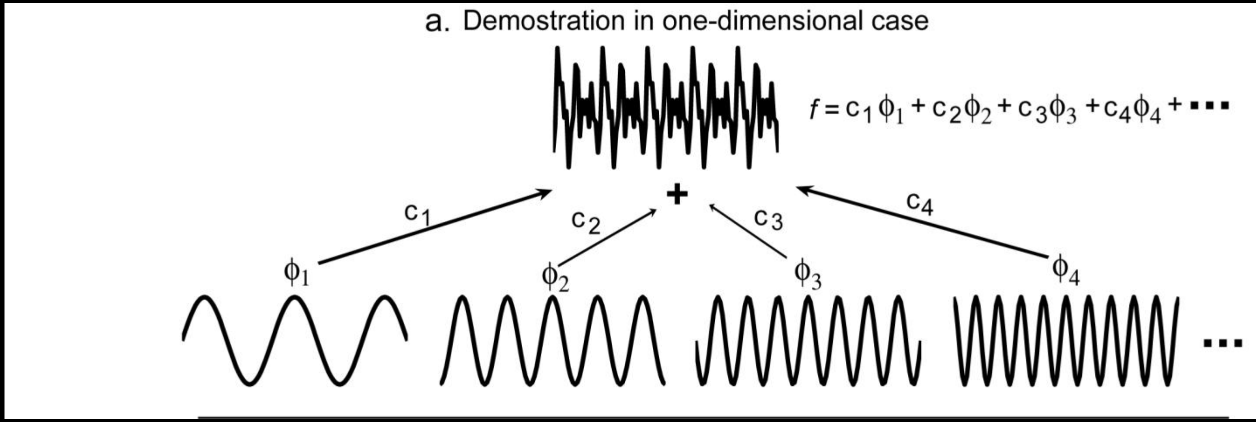

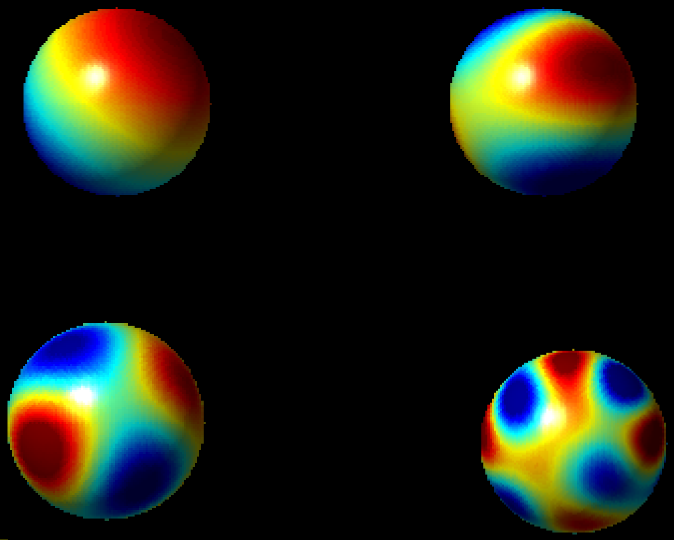

Spherical Harmonics: one example Laplace-Beltrami basis for the sphere.

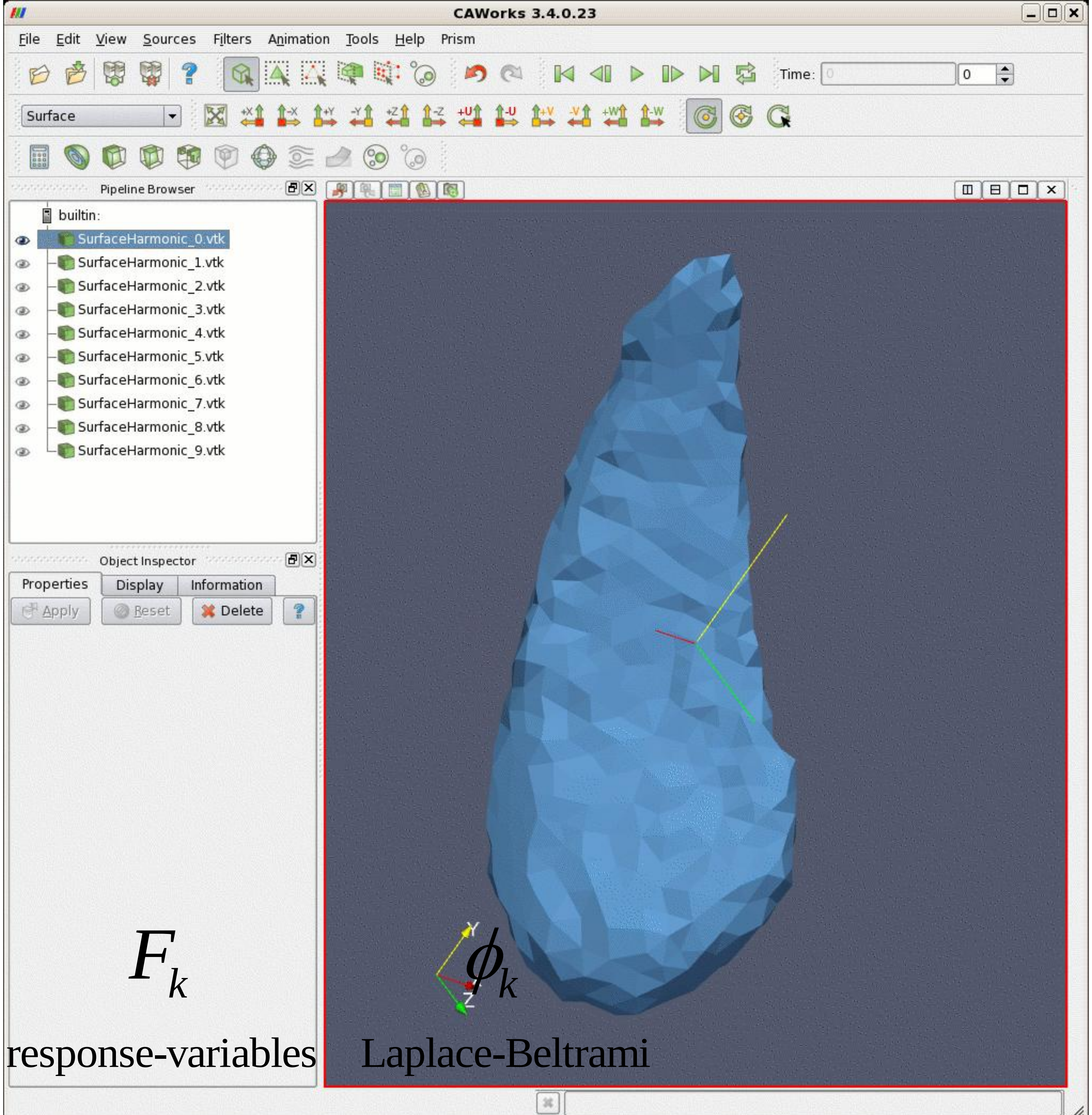

$$F = \sum_k F_k \phi_k$$

response-variables Laplace-Beltrami

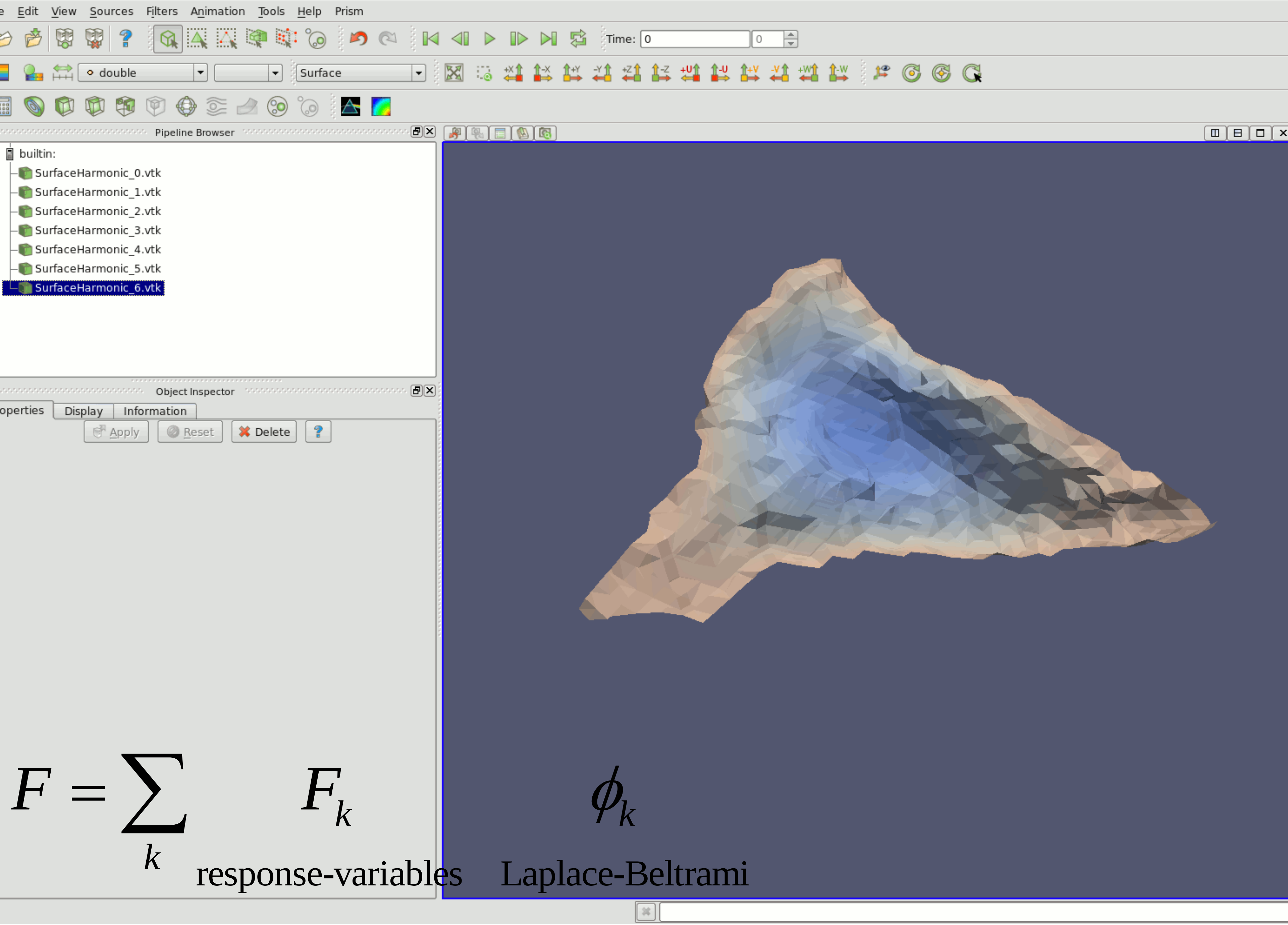

$$F = \sum_k F_k \phi_k$$

response-variables Laplace-Beltrami

Laplace-Beltrami Orthonormal Base

$$F = \sum_k F_k \phi_k$$

response-variables Laplace-Beltrami

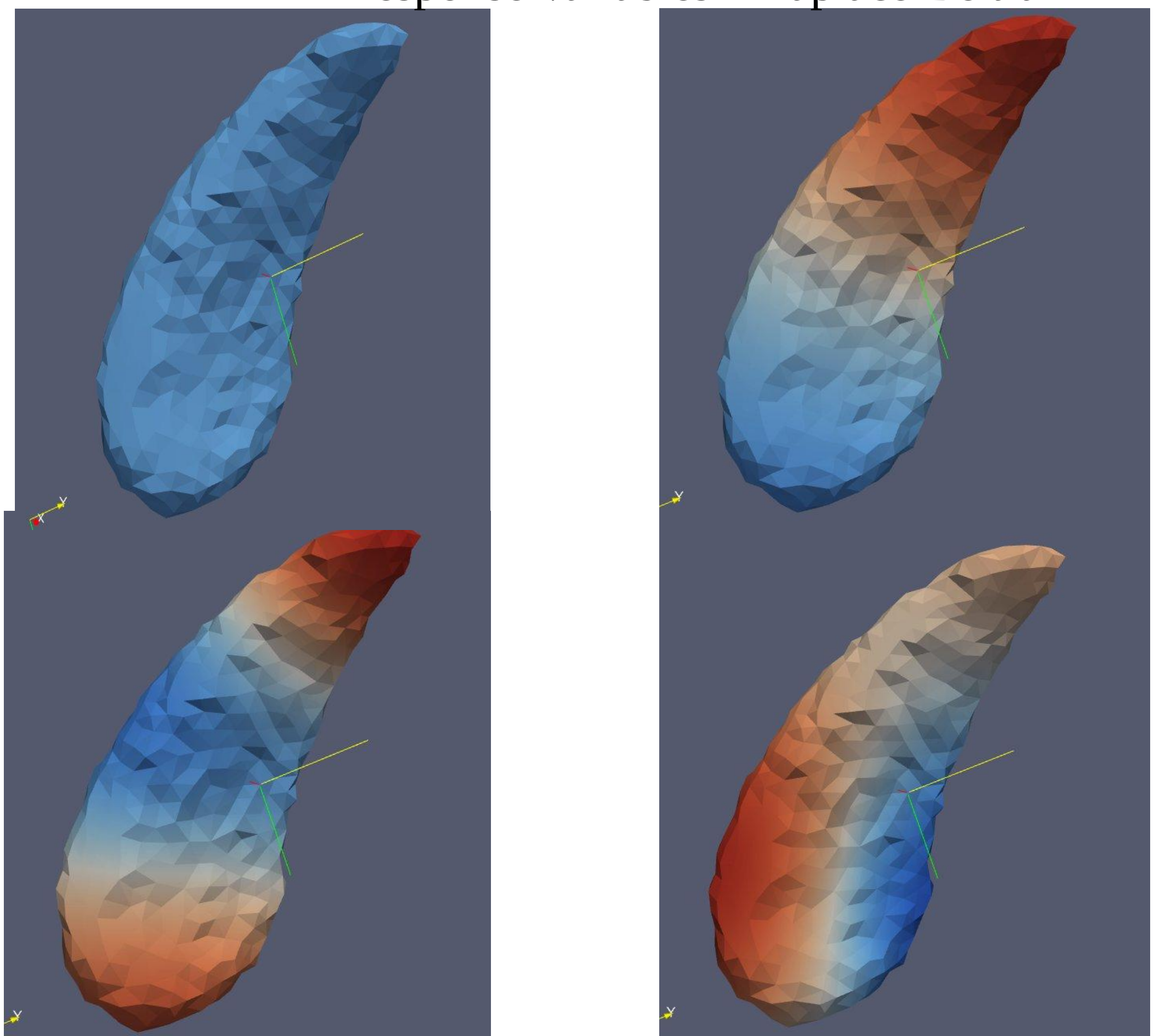

Laplace-Beltrami Surface Basis

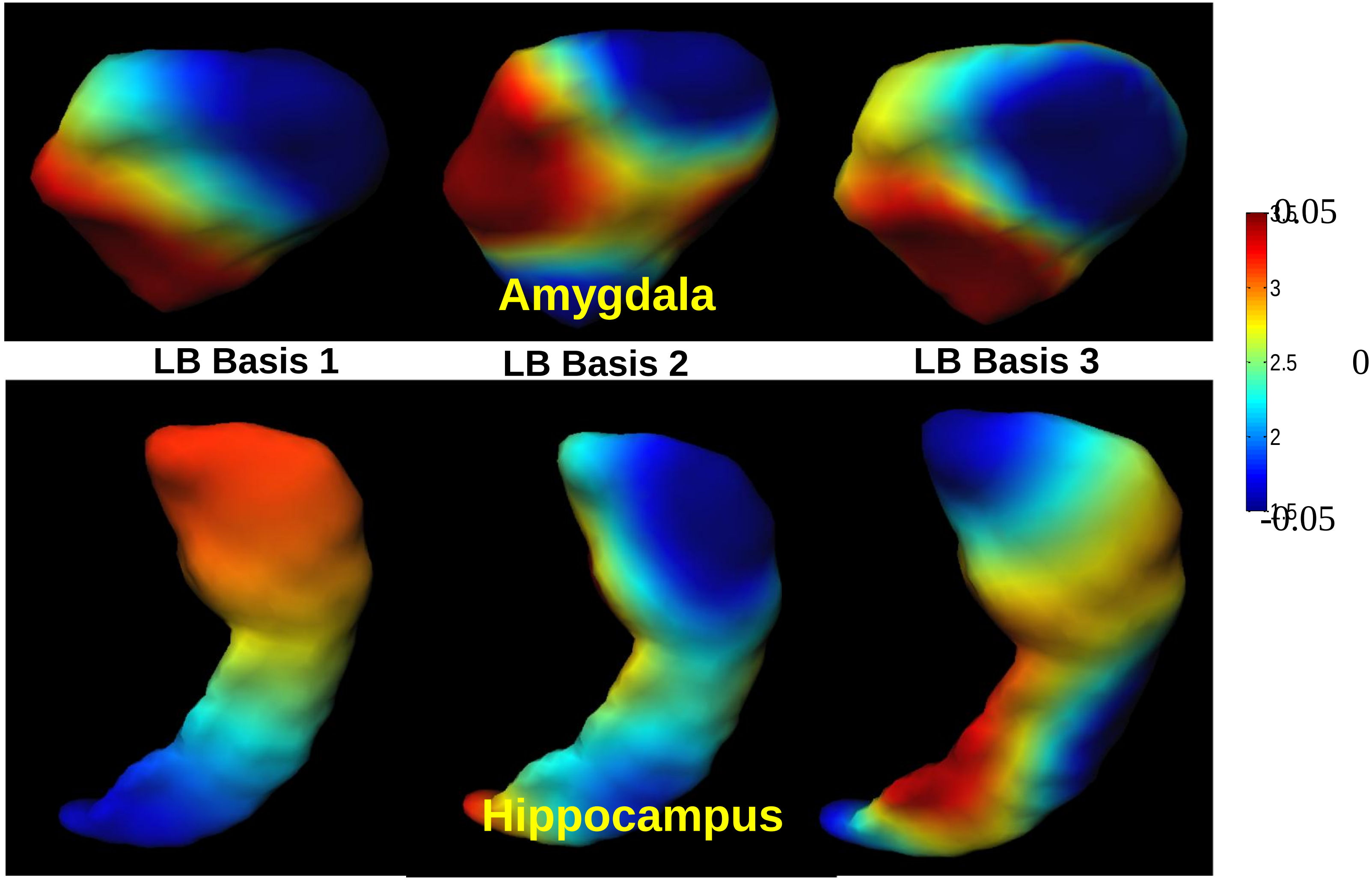

$$F = \sum_k \quad F_k \quad \phi_k$$

response-variables Laplace-Beltrami

Atrophy patterns: PREDICT

Rank sum tests thresholded at 5% family-wise significance (significant regions in red)

Younes, Paulsen, Ross, et. All.,Heterogeneous atrophy of subcortical structures in prodromal HD as revealed by statistical shape analysis, submitted.

Atrophy pattern: Left Putamen

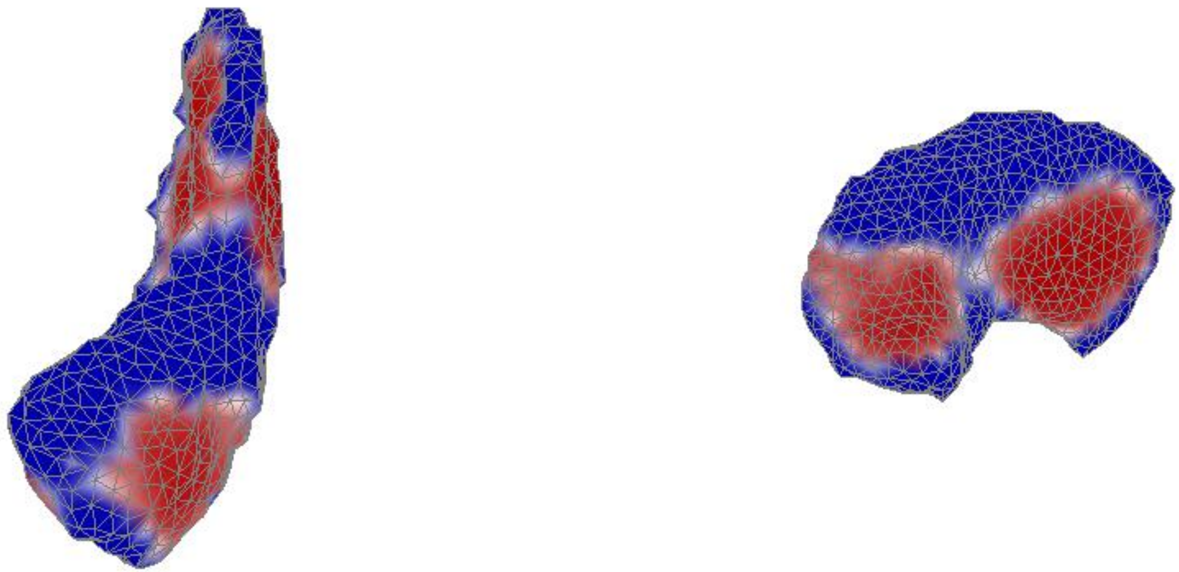

Two views of the atrophy pattern estimated on the left putamen

Younes, Paulsen, Ross, et. All.,Heterogeneous atrophy of subcortical structures in prodromal HD as revealed by statistical shape analysis, submitted.

Atrophy pattern: Right Putamen

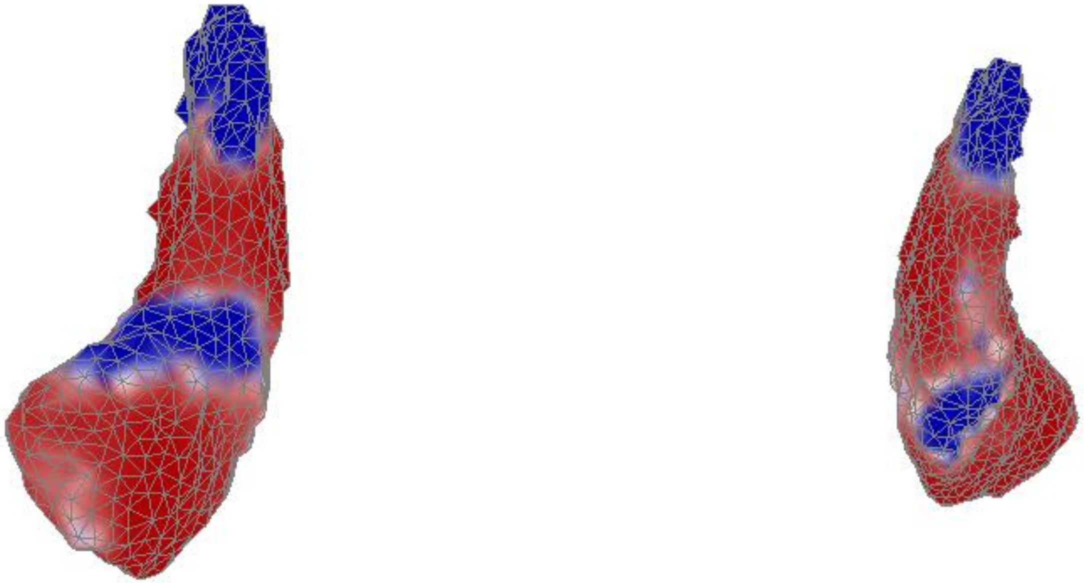

Two views of the atrophy pattern estimated on the right putamen

Younes, Paulsen, Ross, et. All.,Heterogeneous atrophy of subcortical structures in prodromal HD as revealed by statistical shape analysis, submitted.

Atrophy Pattern: Left Caudate

Two views of the atrophy pattern estimated on the left caudate

Younes, Paulsen, Ross, et. All.,Heterogeneous atrophy of subcortical structures in prodromal HD as revealed by statistical shape analysis, submitted.

Atrophy Pattern: Right Caudate

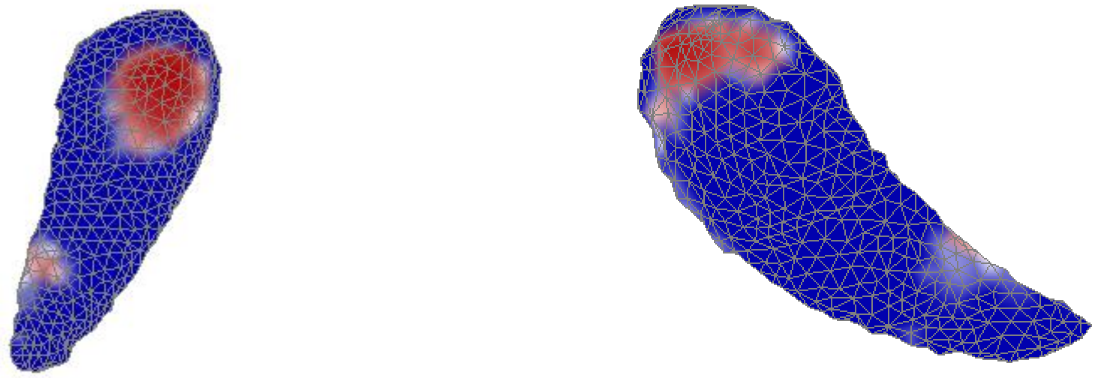

Two views of the atrophy pattern estimated on the right caudate

Younes, Paulsen, Ross, et. All.,Heterogeneous atrophy of subcortical structures in prodromal HD as revealed by statistical shape analysis, submitted.

Clustering

Clustering Based on Significant Discriminating Features

$$F = \sum_{k} \underset{Features}{F_k} \;\; \phi_k$$

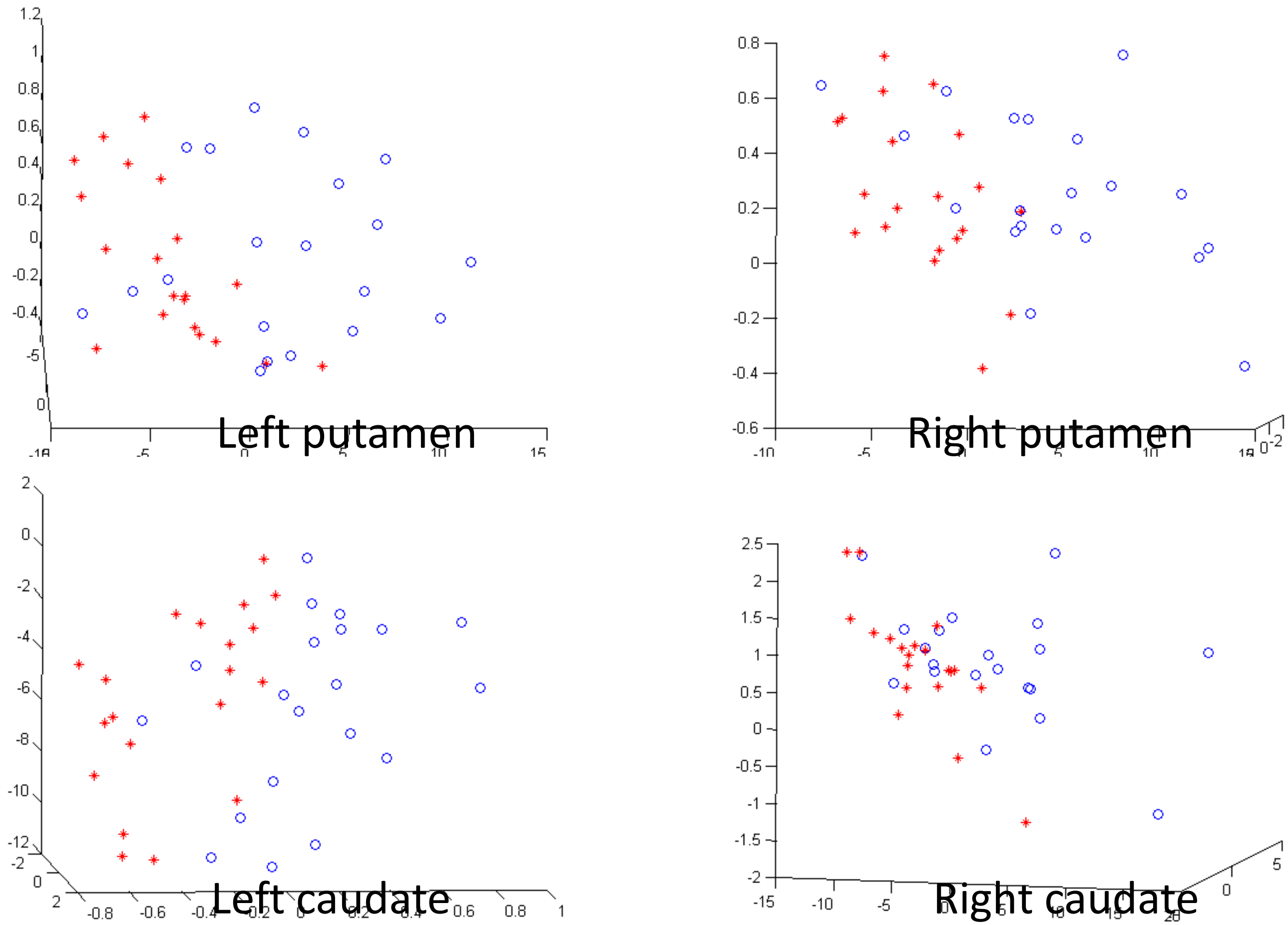

Statistical Significance

P-values

	Left putamen	Right putamen	Left Caudate	Right Caudate
Volume	0.0006	0.00005	0.0066	0.0031
Jacobian	<0.0001	.0001	0.011	.0015
Jacobian centered	.0011	.0003	.0014	.043
Tangential atrophy	0.0005	<0.0001	0.005	0.0004
Centered T. atrophy	0.094	0.0012	0.0001	0.0024
Jacobian on harmonics	.0005	.0001	<.0001	.035
PCA on momentum	.0011	.001	.0034	0.0088
PCA on jacobian	.0004	<.0001	.0012	.0013

p-value accuracy: .0001

Younes, Paulsen, Ross, et. All.,Heterogeneous atrophy of subcortical structures in prodromal HD as revealed by statistical shape analysis, submitted.

The Locality of Shape Change in ADHD

ADHD: Basal Ganglia Shape Analysis

	N	gender		Age(SD)
		Female	Male	
CON	66	31	35	10.5 (1.3)
ADHD	47	20	27	10.4 (1.2)

Basal Ganglia Template

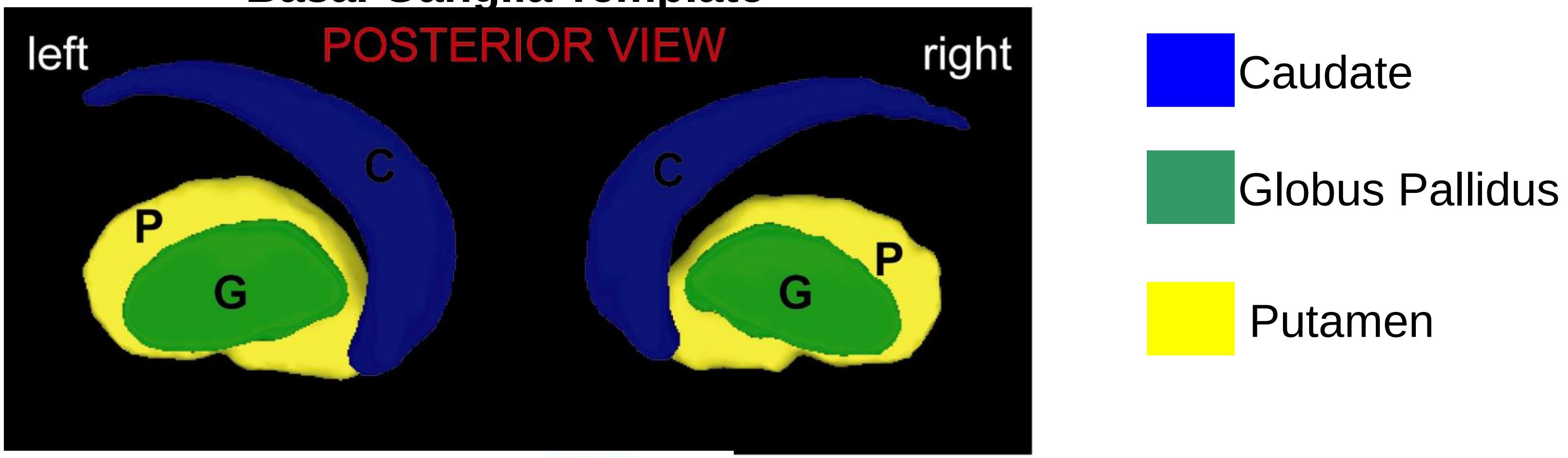

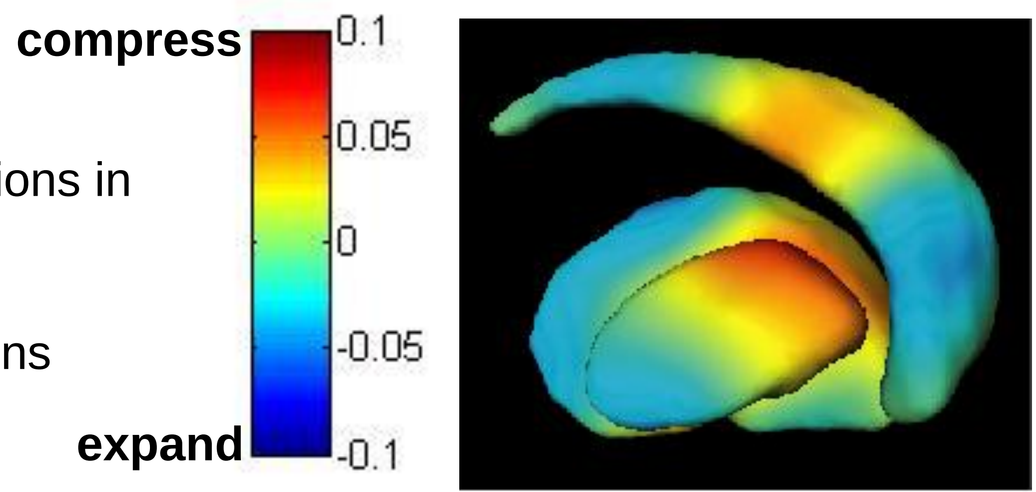

Reconstructions in statistically significant Eigenfunctions $p<.05$

Qui A, Crocetti D, Adler M, Mahone EM, Denckla M, Miller MI, Mostofsky SH (2009) Basal Ganglia Volume and Shape in Children With Attention Deficit Hyperactivity Disorder. Am. J. Psychiatry. 166: 74-82.

Subcortical Shape Analysis in Dementia

Groups	N	gender		age (mean±SD)
		male	female	
control	133	71	62	75.8±4.90
MCI	170	119	51	74.6±7.39
AD	80	49	31	75.2±7.62

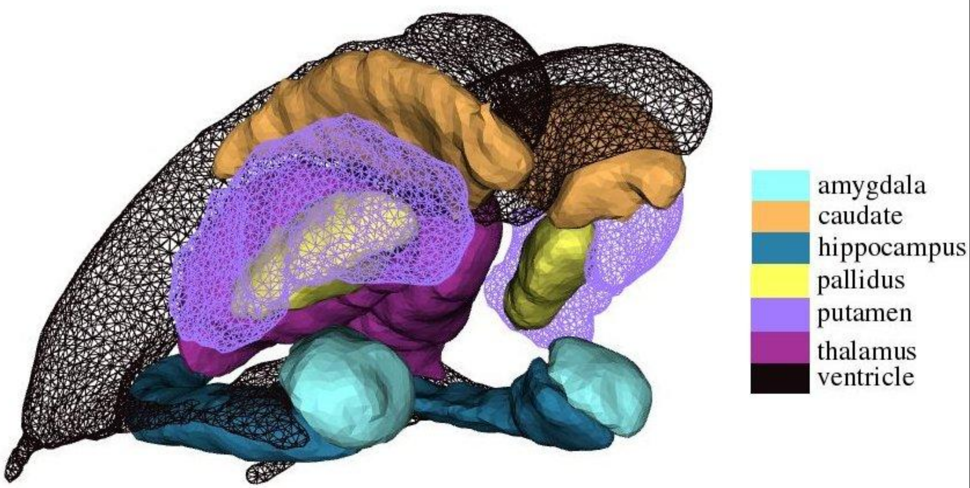

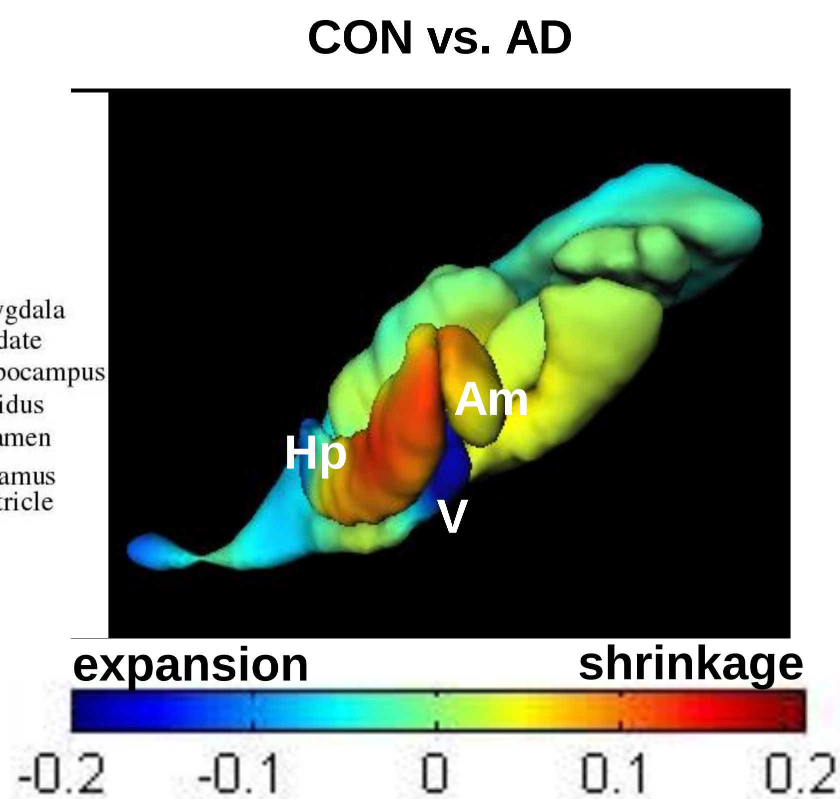

Reconstructions in statistically significant $p<.05$

Anqi Qiu Christine Fennema Notestine, Anders M. Dale, Michael I. Miller, and the Alzheimer's Disease Neuroimaging Initiative, "Regional Subcortical Shape Abnormalities in Mild Cognitive Impairment and Alzheimer's Disease ", NeuroImage,45:656-661, 2009

The End